Ultrafast nonlinear optical response of strongly correlated systems: Dynamics in the quantum Hall effect regime

A. T. Karathanos and I. E. Perakis
Department of Physics, University of Crete, P. O. Box 2208, 710 03, Heraklion, Crete, Greece

N. A. Fromer and D. S. Chemla
Department of Physics, University of California, Berkeley, California 94720
and Materials Science Division, Lawrence Berkeley National Laboratory, Berkeley, California 94720
(Received 18 June 2002; revised manuscript received 9 October 2002; published 21 January 2003)

We present a theoretical formulation of the coherent ultrafast nonlinear optical response of a strongly correlated system and discuss an example where the Coulomb correlations dominate. We separate out the correlated contributions to the third-order nonlinear polarization, and identify non-Markovian dephasing effects coming from the noninstantaneous interactions and propagation in time of the collective excitations of the many-body system. We discuss the signatures, in the time and frequency dependence of the four-wave-mixing (FWM) spectrum, of the inter-Landau level magnetoplasmon excitations of the two-dimensional electron gas in a perpendicular magnetic field. We predict a resonant enhancement of the lowest Landau-level (LL) FWM signal, a strong non-Markovian dephasing of the next LL magnetoexciton (X), a symmetric FWM temporal profile, and strong oscillations as a function of time delay, of quantum kinetic origin. We show that the correlation effects can be controlled experimentally by tuning the central frequency of the optical excitation between the two lowest LL's.

DOI: 10.1103/PhysRevB.67.035316 PACS number(s): 71.10.Ca, 71.45.−d, 78.20.Bh, 78.47.+p

I. INTRODUCTION

The properties of systems far from equilibrium and, in particular, the role of many-body and collective effects on the femtosecond and the nanometer scale present relatively unexplored frontiers of condensed-matter physics.[1–5] Such problems are particularly challenging in semiconductors, where the time intervals of interest are often shorter than the interaction times and oscillation periods of the elementary excitations.[1,2,6,7] Examples of well-established pictures for the interaction processes that need to be revised in this regime include the semiclassical Boltzmann picture of point-like particles experiencing instantaneous collisions and the thermal bath pictures of relaxation and dephasing.[2,6,7] Even the notion of weakly interacting ''quasiparticles,'' a cornerstone of condensed-matter physics, must be revisited when describing the ultrafast nonlinear optical response.[1]

Wave-mixing experiments are ideally suited for exploring quantum coherence and collective and correlation effects in semiconductor nanostructures.[1–3] Time-dependent interactions and correlations dominate the four-wave-mixing (FWM) signal during negative time delays, where the Pauli blocking effects vanish.[1,2] The treatment of such interactions within the time-dependent Hartree-Fock (HF) approximation[5] predicts an *asymmetric* temporal profile of the FWM signal.[1–3] The negative time delay signal generated by mean-field exciton-exciton interactions decays twice as fast as the positive time delay signal. The observation of strong deviations from this asymmetric HF temporal profile in undoped semiconductors was attributed to exciton-exciton correlations.[1,2]

The importance of many-body effects in determining the time and frequency profile of the ultrafast nonlinear optical spectra may be traced microscopically to the coupling, via the interactions, of the one-particle density matrix that describes the optical polarization measured in the experiment to many-particle correlation functions (e.g. the higher density matrices).[2,4,8] The latter are factorized within the time-dependent HF approximation.[5] The correlation-induced fluctuations, described by the deviations from the factorized form, generate a new FWM signal, which can display a distinct time and frequency dependence as compared to the mean-field signal. Such correlation effects are most pronounced during time scales shorter than the characteristic times associated with the interaction processes.[2,9]

To describe the above nonequilibrium many-body effects, one must use a controlled truncation of the infinite hierarchy of coupled density matrix or Green's function equations. In undoped semiconductors, this hierarchy truncates if one adopts an expansion in terms of the optical fields.[4,8–12] This is the case since (a) in the ground state, the conduction band is empty and the valence band is full, and (b) the Coulomb-induced coupling of the conduction and valence bands via, e.g., Auger-like processes is negligible: in the absence of optical fields, the numbers of conduction-band electrons and valence-band holes are independently conserved. In undoped semiconductors, the lowest electronic excitations of the ground-state electrons are the high-energy interband e-h pairs, which can adjust almost instantaneously to the dynamics of the photoexcited carriers.[13] The photoexcited e-h pairs then behave as quasiparticles with mutual interactions, while the ground state can be considered as rigid. In this case, the many-body nature of the system only affects the different parameters associated with the band structure and the dielectric screening,[14] and the only Coulomb correlations that require consideration are dynamically generated by the optical excitation.[8] The almost unexplored dynamics of strongly correlated systems, whose ground-state electrons interact un-

adiabatically with the photoexcited *e-h* pairs, raises very fundamental questions.

A widely used theoretical approach for treating the above many-body effects in undoped semiconductors is the ''dynamics-controlled truncation scheme'' (DCTS).[8,10,11,15] In this theory, the response of the semiconductor is expanded in terms of the number of created *e-h* pairs. Importantly, the Coulomb interactions that contribute to a specified order in the applied field only occur between such *e-h* pairs. This is the case since there is the correspondence between the number of *e-h* pairs and the sequence of photon absorption and emission, and there are no carriers in the ground state to interact with the photoexcited carriers. The latter condition is not met, however, in doped quantum wells, where a correlated two-dimensional electron gas (2DEG) is present in the ground state, and the DCTS fails there.[11] A new method that extends the DCTS principles to systems with a strongly correlated ground state is required. In a series of works we applied a theory based on a canonical transformation and time-dependent coherent states to study the case where the interactions between the photoexcited *e-h* pairs and the electron Fermi sea (FS) excitations dominate the coherent nonlinear optical response.[9,16,17]

In FS systems, the direct exciton-exciton interactions, which dominate the nonlinear response in undoped semiconductors, are screened, and the nonlinear response is determined by the FS excitations. For resonant photoexcitation, the optical dynamics is dominated by inelastic electron-electron (e-e) scattering processes.[18,19] At low temperatures, the dephasing times close to the Fermi edge increase by a few picoseconds, in agreement with Fermi liquid theory.[18] For *below-resonance* excitation, however, the dissipation processes are suppressed and coherent effects dominate. A novel dynamics of the Fermi edge singularity is then observed,[16,20] due to many-body correlations of the photoexcited holes with the FS excitations.[9,17,20]

In the absence of long-lived excitations, a many-particle system, such as a FS, interacts with the photoexcited *e-h* pairs almost instantaneously, i.e., during time scales shorter than the pulse duration. The system then behaves to first approximation as a thermal bath, and its interactions with the photoexcited carriers can be treated within the dephasing and relaxation time approximations. This is not the case, however, if the duration of the interactions is comparable to or longer than the measurement times.[17] In the latter case, the semiclassical instantaneous collision picture breaks down, and quantum-mechanical interference effects lead to nonexponential decay and non-Markovian memory effects.[2,6,7,21] To study dephasing in the above quantum kinetic regime, one must account for the time evolution of the *coupled* photoexcited carrier–FS system.[9,17]

The change in the energy spectrum caused by a perpendicular magnetic field restricts the phase space available for *e-e* scattering in doped quantum wells (QW's).[22] For strong magnetic fields, the Coulomb correlations are enhanced due to the suppression of the kinetic energy.[23] In the quantum Hall effect (QHE) regime,[23,24] long-lived collective excitations dominate the 2DEG spectrum.[25–28] Recently, the first experimental studies of the role of such collective excitations in the ultrafast nonlinear optical dynamics were reported.[29–31] The presence of low-energy excitations and the strongly correlated ground state raise formidable theoretical difficulties for describing the dephasing dynamics of the 2DEG.

We are interested in developing a theoretical framework for describing the ultrafast dephasing and the nonlinear optical response of strongly correlated systems. Examples of systems of interest include modulation-doped semiconductor QW's, where different strongly correlated ground-states are realized in the QHE regime, and the ferromagnetic semiconductors doped with magnetic impurities. In the first part of the paper (Secs. II–V) we describe the third-order nonlinear optical response of a many-electron two-band system without assuming a HF or other specific ground state. In the second part (Secs. VI and VII) we study the role of the inter–Landau-Level (inter-LL) magnetoplasmon (MP) collective excitations in the transient FWM spectrum of the cold 2DEG. Here we concentrate on filling factors close to $\nu = 1$, where the spin-$\uparrow$ ground-state electrons lead to ferromagnetic properties (QHE ferromagnet), and the excitation spectrum is governed by strong Coulomb correlations.[32–34] We consider photoexcitation with σ_+ circularly polarized light, in which case only spin-$\downarrow$ electrons are excited and the MP collective excitations play the most important role.[30] Our results explain the most salient qualitative features of the transient FWM spectrum observed in recent experiments.[30]

Our theory applies to a two-band system described by a Hamiltonian that independently conserves the number of conduction-band electrons and valence-band holes, e.g., the GaAs/AlGaAs QW's.[5] We describe the coupling to the optical field within the dipole approximation, and neglect any stimulated emission. We consider zero temperature, which is adequate for describing correlations that require thermal energies smaller than the excitation and interaction energies of the system in order to be observed. The third-order polarization calculated here is expected to describe the nonlinear optical signal when the photoexcited carrier density is smaller than the density of the ground-state electrons, in which case the cold 2DEG correlations prevail.

The outline of the paper is as follows. In Sec. II we set up the general problem and discuss the nature of the states that contribute to the optical spectra. In Sec. III we study the time evolution of the system, and introduce a decomposition of the photoexcited many-body states, which allows us to classify the different interaction contributions. In Sec. IV we use the above decomposition to derive the equation of motion for the third-order nonlinear polarization, Eq. (37). The decompositions introduced in Sec. III allow us to distinguish the coherent and excitonic effects from the incoherent effects, and separate out the factorizable from the correlated nonlinear polarization contributions even in the case of a strongly correlated ground-state. In Sec. V we discuss an example of a basis of strongly correlated states that can be used to obtain equations of motion for the correlation functions that describe the many-body effects. In Sec. VI we derive a generalized average polarization model[2,15,36,37] that we use to identify the signatures of the collective 2DEG excitations in the time-dependent FWM spectra. The ground-state correlations

determine the interaction parameters in the equations of motion. We derive in the Appendixes a number of relations among such interaction parameters that are imposed by the electron-hole symmetry of the ideal 2DEG. In Sec. VII we present numerical results that describe the correlation-induced ultrafast dynamics predicted by the above model. We identify a number of interesting features in the time-dependent FWM spectrum, which arise from the propagation in time of the inter-LL MP's and their noninstantaneous interactions with the photoexcited excitons. We end with the conclusions.

II. PROBLEM SETUP

We are interested in developing a comprehensive approach to the problem of the nonlinear optical response in the case of photoexcitation from the valence to the conduction band. Within the dipole approximation, the coupling to the optical field can be described by the Hamiltonian[5] ($\hbar=1$)

$$H_{\rm tot}(t)=H-\mu\mathcal{E}(t)\hat{X}^{\dagger}-\mu\mathcal{E}^{*}(t)\hat{X}. \tag{1}$$

In the above equation, H is the ''bare'' many-body Hamiltonian that describes the band-structure effects and the interactions, $\mathcal{E}(t)$ is the applied optical field, $\hat{X}$ is the optical transition operator, and μ is the interband transition matrix element. In the case of a semiconductor QW containing a 2DEG in a magnetic field, the Hamiltonian H has the form[5]

$$H=\sum_{i,k}\,[E_g+\Omega_c^c(i+1/2)]\hat{e}_{k,i}^{\dagger}\hat{e}_{k,i} + \sum_{i,k}\,\Omega_c^v(i+1/2)\hat{h}_{-k,i}^{\dagger}\hat{h}_{-k,i}+V_{ee}+V_{hh}+V_{eh}, \tag{2}$$

where E_g is the band gap, and V_{ee}, V_{eh}, and V_{hh} are, respectively, the e-e, e-h, and h-h interactions (see Appendix A). The magnetic field splits the conduction and valence bands into discrete electron (e) and hole (h) LL's, e-LLi and h-LLi, where i includes both the LL index and the spin. $\hat{e}_{k,i}^{\dagger}$ is the creation operator of the LLi conduction-band electron, with cyclotron energy Ω_c^c, and $\hat{h}_{k,i}^{\dagger}$ is the creation operator of the LLi valence-band hole, with cyclotron energy Ω_c^v (see Appendix A).[26] The optical transition operator $\hat{X}^{\dagger}$ is expanded in terms of interband e-h pair creation operators $\hat{X}_i^{\dagger}$ that we refer to as the exciton (X) operators from now on:

$$\hat{X}^{\dagger}=\sum_i\,\sqrt{N_i}\hat{X}_i^{\dagger}. \tag{3}$$

In the case of the 2DEG in a magnetic field, it is convenient to introduce the LLi magnetoexciton states $|X_i\rangle=\hat{X}_i^{\dagger}|0\rangle$, where $|0\rangle$ is the ground eigenstate of the many-body Hamiltonian H, with full valence band and the 2DEG at rest. The eigenvalue equation $H|0\rangle=0$ defines the ground-state energy as the reference point. In the ideal system,

$$\hat{X}_i^{\dagger}=\frac{1}{\sqrt{N_i}}\sum_k\,\hat{e}_{k,i}^{\dagger}\hat{h}_{-k,i}^{\dagger}, \tag{4}$$

where $N_i=N(1-\nu_i)$, with $N=L^2/2\pi l^2$ being the LL degeneracy, l the magnetic length, L the system size, and

$$\nu_i=\frac{1}{N}\sum_k\,\langle 0|\hat{e}_{k,i}^{\dagger}\hat{e}_{k,i}|0\rangle \tag{5}$$

gives the filling of LLi in the absence of optical excitation. Note that the exciton states $|X_i\rangle$ are strongly correlated: they are created by the operator $\hat{X}_i^{\dagger}$ acting on the ground eigenstate of the many-body Hamiltonian H, which describes the correlated electron gas at rest. From Eq. (4) we obtain the commutation relation

$$[\hat{X}_i,\hat{X}_j^{\dagger}]=\delta_{ij}\left(1-\frac{\Delta\hat{N}_i}{N_i}\right), \tag{6}$$

where the operator

$$\Delta\hat{N}_i=\sum_k\,(\hat{h}_{-k,i}^{\dagger}\hat{h}_{-k,i}+\hat{e}_{k,i}^{\dagger}\hat{e}_{k,i})-N\nu_i, \tag{7}$$

with $\langle 0|\Delta\hat{N}_i|0\rangle=0$, describes the number of photoexcited carriers in LLi.

The optical spectra are determined by the polarization of the photoexcited system,

$$P(t)=\mu\langle\psi|\hat{X}|\psi\rangle=\mu\sum_i\,\sqrt{N_i}P_i(t), \tag{8}$$

where P_i are the average values of the exciton operators,

$$P_i(t)=\langle\psi|\hat{X}_i|\psi\rangle. \tag{9}$$

The state $|\psi(t)\rangle$ evolves from the state of the system prior to the optical excitation according to the Schrödinger equation for the Hamiltonian $H_{tot}(t)$. For zero temperature, this initial state is the lowest many-body eigenstate $|0\rangle$ and describes all correlations in the absence of optical fields.

As in the theoretical approaches of Refs. 11 and 12, there is a one-to-one correspondence between the photon absorption/emission and the e-h pair creation/destruction. Since an electron gas may be present in the ground-state, we classify the photoexcited states in terms of the number of valence-band holes, i.e., the number of missing valence-band electrons as compared to the ground-state $|0\rangle$. We thus decompose the optically excited state $|\psi\rangle$ as

$$|\psi\rangle=|\psi_0\rangle+|\psi_1\rangle+|\psi_2\rangle, \tag{10}$$

where $|\psi_n\rangle$ is the *collective* n-h photoexcited state. The above holes interact strongly with the 2DEG.[34] Note that the states with $n\geqslant 3$ do not contribute to the third-order nonlinear polarization.[4]

Substituting Eq. (10) into the Schrödinger equation for the Hamiltonian $H_{tot}(t)$, we obtain up to third order in the optical field that

$$i\partial_t|\psi_0\rangle-H|\psi_0\rangle=-\mu\mathcal{E}^{*}\hat{X}|\psi_1\rangle, \tag{11}$$

$$i\partial_t|\psi_1\rangle-H|\psi_1\rangle=-\mu\mathcal{E}\hat{X}^{\dagger}|\psi_0\rangle-\mu\mathcal{E}^{*}\hat{X}|\psi_2\rangle, \tag{12}$$

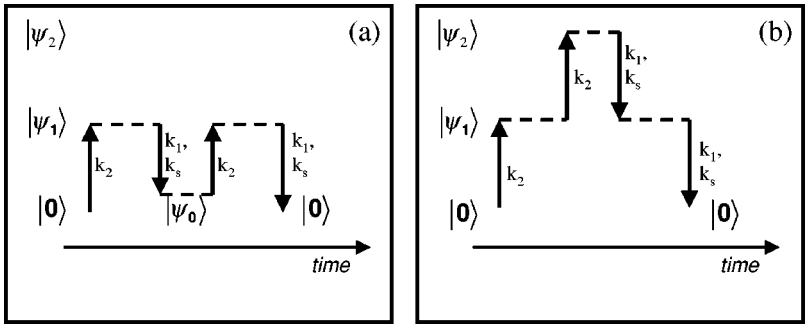

FIG. 1. Photoexcitation of the intermediate (a) $0-h$, $|\psi_0\rangle$, and (b) $2-h$, $|\psi_2\rangle$, states via the nonlinear optical processes that contribute to the FWM spectrum. To third order in the optical fields, the coherent emission of a k_s photon in the FWM direction $k_s=2k_2-k_1$ is determined by the excitation of two e-h pairs by the optical field k_2, and the deexcitation of one e-h pair by the optical field k_1. Although in a coherent FWM experiment we must begin and end the nonlinear excitation process with the system in its ground state, the intermediate $0-h$ state does not need to be the ground-state $|0\rangle$, but can contain electron-gas excitations. The above optical transitions are assisted by Coulomb interactions, which lead to the correlations discussed in Sec. III.

$$i\partial_t|\psi_2\rangle - H|\psi_2\rangle = -\mu\mathcal{E}\hat{X}^\dagger|\psi_1\rangle, \tag{13}$$

with initial condition $|\psi_n(-\infty)\rangle=\delta_{n,0}|0\rangle$, where the Hamiltonian H includes the degrees of freedom which lead to the dephasing. The physics of the above equations is clearly displayed: $|\psi_0\rangle$ is coupled to $|\psi_1\rangle$ by the destruction of one e-h pair, $|\psi_1\rangle$ is coupled to $|\psi_2\rangle$ by the destruction of one e-h pair and to $|\psi_0\rangle$ by the creation of one e-h pair, and $|\psi_2\rangle$ is coupled to $|\psi_1\rangle$ by the creation of one e-h pair. Figure 1 shows the optical transitions that determine the FWM signal up to third order in the optical field. It is worth noting that, by retaining in the expansion, Eq. (10), states with higher h numbers, one can extend Eqs. (11)–(13) to treat higher order nonlinear processes.

Even if we restrict ourselves to the electronic degrees of freedom, the Hilbert space of states that determine the ultrafast nonlinear response of a doped QW is complicated. Strictly speaking, it contains all the states that can be generated through the coupling of e-h pairs photoexcited in any of the QW subbands with all the excitations of the 2DEG: plasmons, magnons, incoherent pairs, etc. For the purpose of developing an intuitive picture of the important physical processes, it is useful to first discuss qualitatively the ensemble of states that are most relevant to the problem at hand.

For the experimental conditions considered in the second part of the paper, the most important 2DEG excitations are the collective inter-LL MP modes that arise from the coherent promotion of a LL0 electron to a higher LL.[25,26] Such MP eigenstates are well approximated by the form[23]

$$|M_{\mathbf{q}}\rangle=\sum_{kjj'}\rho_{jj'}(\mathbf{q})\hat{e}^\dagger_{k+q_y,j}\hat{e}_{k,j'}|0\rangle, \tag{14}$$

where $|0\rangle$ is the strongly correlated ground state and the amplitudes $\rho_{jj'}(\mathbf{q})$ are related to the LL$j'\rightarrow$ LLj contribution to the density operator. Note that, similar to the exciton states $|X_i\rangle$, the above MP states are strongly correlated. For the magnetic fields of interest, in the ground state $|0\rangle$, only e-LL0 is partially filled with the 2DEG at rest, while all the h-LL states are empty (full valence band). Since we focus on photoexcitation of the LL0 and LL1 optical transitions, the main contribution to the optical spectra comes from the resonant LL0→LL1 MP's, whose energy is close to the LL0→LL1 energy.[25,26]

It is useful to make the junction with two domains well studied in the recent literature: photoexcited undoped QW, and 2DEG in the QHE regime. One can distinguish between the excitations of two subsystems: (i) the QW interband excitations (with the 2DEG at rest), which consist of $1e$-h, $2e$-h, ... pairs created in the different QW LL's, and (ii) the 2DEG excitations (with unexcited QW and full valence band), i.e., the 1-MP, 2-MP, ... states, etc. The ensemble of states that determine the third-order nonlinear optical spectra can then be thought as consisting of ℓ e-h pairs, $l\leqslant 2$, and n 2DEG excitations. For photoexcitation of the LL0 and LL1 exciton transitions, the inter-LL MP provides a resonant coupling of the two LL's, since its energy is comparable to the LL0 $\rightarrow$ LL1 excitation energy. In contrast, the LLi exciton states with $i\geqslant 3$, the states with $n\geqslant 2$ MP's, and the continuum of incoherent 2DEG pair excitations analogous to the ones in an ordinary Fermi liquid[23] contribute to the optical spectra via nonresonant processes.

One can draw an analogy between the X-MP effects of interest here and the X-phonon interaction effects studied in undoped semiconductors.[6–8,11,21,39] However, there are some important differences. In the undoped system, the electronic operators commute with the collective excitation (phonon) operators, and the ground-state correlations can be neglected. One can then expand the state $|\psi\rangle$ in terms of a basis consisting of products of phonon wave functions times e-h pair two-particle wave functions. In contrast, a MP is an electronic excitation [see Eq. (14)], and its creation operator may not commute with other electronic operators. Pauli exchange effects must then be considered, while, unlike for phonons, MP's do not strictly obey Bose-Einstein statistics. Importantly, one must treat the strong correlations of the ground-state electrons. Issues such as the above complicate the use of a simple basis to calculate the nonlinear optical response of the 2DEG. In Sec. V we discuss an example of a strongly correlated basis set that can be used to address the above issues. An important advantage of this particular basis is that

it facilitates the development of a simple model that describes the most salient dynamical features of the ultrafast nonlinear optical spectra.

III. TIME-DEPENDENT INTERACTION EFFECTS

In this section we consider the time evolution of the coupled photoexcited carrier–2DEG system that leads to the dephasing of the *e*-*h* polarization. We are mainly interested in dephasing due to electronic degrees of freedom, and thus the distinction between the photoexcited carriers and the ''bath'' excitations is less clear as compared, e.g., to the case of a phonon bath. We address this issue by separating out the excitonic contribution directly excited by the optical field (2DEG at rest) from the contribution of the excited 2DEG configurations (denoted by 2DEG* from now on) that lead to the dephasing. For this we decompose the $1-h$ photoexcited state as follows:

$$|\psi_1\rangle=\sum_i P_i^L|X_i\rangle+|\bar{\psi}_1\rangle, \tag{15}$$

where $|\bar{\psi}_1\rangle$ is the $\{1-h/2\text{DEG}^*\}$ contribution defined by the condition $\langle X_i|\bar{\psi}_1\rangle=0$, and the exciton amplitude

$$P_i^L=\langle X_i|\psi_1\rangle=\langle 0|\hat{X}_i|\psi\rangle \tag{16}$$

reduces to the linear polarization to first order in the optical field. To describe the two-photon nonlinear optical processes in Fig. 1, we must consider, in addition to the X-2DEG interactions, the X-X and X-$|\bar{\psi}_1\rangle$ interactions during the optical transitions. For this we first separate out the total interaction contribution to the $2-h$ and $0-h$ intermediate states, $|\psi_2\rangle$ and $|\psi_0\rangle$, respectively, and then identify the particular contributions due to the interactions among the above 1-*h* excitations that lead to the correlation effects:

$$|\psi_2\rangle=\frac{1}{2}\sum_{ii'} P_i^L P_{i'}^L|X_iX_{i'}\rangle+|\psi_2^{int}\rangle,$$

$$|\psi_2^{int}\rangle=\sum_i P_i^L\hat{X}_i^\dagger|\bar{\psi}_1\rangle+|\bar{\psi}_2\rangle, \tag{17}$$

where the state $|X_iX_{i'}\rangle=\hat{X}_i^\dagger\hat{X}_{i'}^\dagger|0\rangle$ describes two noninteracting X's, and

$$|\psi_0\rangle=\langle 0|\psi\rangle|0\rangle+|\psi_0^{int}\rangle,$$

$$|\psi_0^{int}\rangle=-\sum_i P_i^{L*}\hat{X}_i|\bar{\psi}_1\rangle+|\bar{\psi}_0\rangle, \tag{18}$$

where we have separated out the ground-state contribution from the 2DEG* contributions by requiring that $\langle 0|\psi_0^{int}\rangle=\langle 0|\bar{\psi}_0\rangle=0$.

The above decompositions are analogous to the cumulants introduced within the DCTS for the case of undoped semiconductors.[8,11] Such cumulants were obtained by subtracting the factorized contributions from the many-body correlation functions. Note, however, that the method presented below also holds in the case where strongly correlated carriers are present in the ground state, as in the 2DEG case, where the assumptions of the DCTS break down. The decompositions of the states $|\psi_0^{int}\rangle$, $|\psi_2^{int}\rangle$, and $|\psi_1\rangle$ also allow us to separate out, in the equations of motion [Eqs. (11), (12), and (13)], the source terms proportional to the optical field from the source terms proportional to the polarizations P_i^L, which lead to different time dependences. The photoexcited states $|\bar{\psi}_0\rangle$, $|\bar{\psi}_1\rangle$, and $|\bar{\psi}_2\rangle$ describe correlated contributions, whose physical origin will be discussed below.

We now derive the equations of motion of the above photoexcited states, which we will use in the following section to derive the nonlinear polarization equation of motion and separate out the factorizable contributions. It is easiest to start with the 1-*h* time-evolved state. Equation (15) splits this state into excitonic (2DEG at rest) and $\{1-h/2\text{DEG}^*\}$ parts, $P_i^L(t)$ and $|\bar{\psi}_1\rangle$, respectively. The state $|\bar{\psi}_1\rangle$ originates from the X-2DEG scattering during the time evolution of the photoexcited X. To describe such interactions, we consider the action of the Hamiltonian H on the exciton states $|X_i\rangle$. By subtracting all the exciton contributions, the state $H|X_i\rangle$ can be expressed in the form

$$H|X_i\rangle=\Omega_i|X_i\rangle-\sum_{i'\neq i} V_{i'i}|X_{i'}\rangle+|Y_i\rangle, \tag{19}$$

where

$$\Omega_i=\langle X_i|H|X_i\rangle \tag{20}$$

is the X_i energy,

$$V_{i'i}=-\langle X_{i'}|H|X_i\rangle=V_{ii}^* \tag{21}$$

describes the Coulomb-induced coupling of the different X's, and $|Y_i\rangle=\hat{Y}_i^\dagger|0\rangle$, where the operator

$$\hat{Y}_i=[\hat{X}_i,H]-\Omega_i\hat{X}_i+\sum_{i'\neq i} V_{ii'}\hat{X}_i \tag{22}$$

describes the interactions between X_i and the rest of the carriers present in the system.

As one can see by using the above equations, the state $|Y_i\rangle$ is orthogonal to all exciton states $|X_j\rangle$, $\langle Y_i|X_j\rangle=0$, and is therefore the $\{1-h/2\text{DEG}^*\}$ state into which X_i can scatter by interacting with the 2DEG. For the experimental conditions of particular interest here, the most important contribution to $|Y_i\rangle$, Eq. (A17), comes from X-MP states. To see this, let us consider the possible final scattering states of the LL1 exciton X_1. Its LL1 electron can scatter to LL0 by emitting a LL0 $\rightarrow$ LL1 MP, a process shown in Fig. 2. Since the MP energy is close to the *e*-LL0 $\rightarrow$ *e*-LL1 energy spacing, the above scattering process is almost resonant. It therefore provides an efficient decay channel of the LL1 exciton to a $\{1\text{-MP}+1\text{-LL0-}e+1\text{-LL1-}h\}$ four-particle excitation of the ground-state $|0\rangle$. All other allowed scattering processes are nonresonant. The X_1 hole can scatter to LL0 by emitting a MP, which leads to a $\{1\text{-MP}+1\text{-LL0-}e+1\text{-LL1-}h\}$ four-particle excitation. The latter state, however, has energy that is significantly higher, by an amount of the order of $\sim\Omega_c^c$

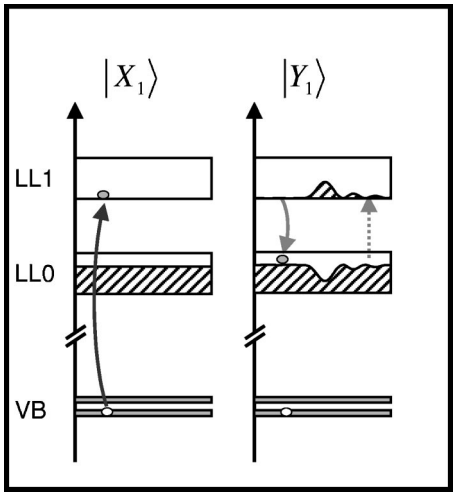

FIG. 2. Photoexcitation of the exciton state, $|X_1\rangle$, and then of the X-MP state $|Y_1\rangle$ via resonant X-2DEG scattering.

$+\Omega_c^v$, from that of the initial X_1 state. Note that, as shown in Appendix A, in the electron-hole symmetric limit the X electron or hole must change LL during the scattering process. In the case of X_0, the LL0 electron can scatter to LL1 by emitting a MP, so that $X_0 \rightarrow \{1\text{-MP}+1\text{-LL0-}e+1\text{-LL1-}h\}$, or the LL1 hole can scatter to LL0, in which case $X_0 \rightarrow \{1\text{-MP}+1\text{-LL0-}e+1\text{-LL1-}h\}$. $|Y_0\rangle$ is thus a linear combination of the same final states as $|Y_1\rangle$. However, in this case the energy of all final states is significantly higher than that of the initial state $|X_0\rangle$. Therefore, the decay of the LL0 exciton is suppressed as compared to that of the LL1 (or higher) exciton. Note that the distinction between resonant and nonresonant interaction processes is most pronounced when the inter-LL excitation energy, of the order of the cyclotron energy exceeds the characteristic 2DEG Coulomb correlation energy $\sim e^2/l$. Expansions in terms of the ratio of the above two energies are known to capture most of the 2DEG correlation effects.[23,25,34]

We now describe the time evolution, to first order in the optical field, of the 1-h photoexcited state $|\psi_1\rangle$. The equation of motion for the linear polarization P_i^L can be derived by projecting the exciton state $\langle X_i|$ to the truncated Eq. (12) and applying Eq. (19):

$$i\partial_t P_i^L = \Omega_i P_i^L - \sum_{i' \neq i} V_{ii'} P_{i'}^L + \overline{P}_i^L - \mu \mathcal{E}(t) N_i^{1/2}. \quad (23)$$

The correlation function

$$\overline{P}_i^L = \langle Y_i|\psi_1\rangle = \langle Y_i|\overline{\psi}_1\rangle, \quad (24)$$

discussed in Sec. V, describes the dephasing of P_i^L and screening effects.

Substituting the decomposition [Eq. (15)] into the Schrödinger equation [Eq. (12)] and using Eqs. (23) and (19), we obtain the equation of motion of the $\{1-h/\text{2DEG}^*\}$ contribution $|\overline{\psi}_1\rangle$:

$$i\partial_t|\overline{\psi}_1\rangle - H|\overline{\psi}_1\rangle = \sum_i [P_i^L|Y_i\rangle - \overline{P}_i^L|X_i]. \quad (25)$$

The operator $P_i^L\hat{Y}_i^\dagger - \overline{P}_i^L\hat{X}_i^\dagger$ also appears in the equation of motion of the $2h$ state. Its first term describes the scattering of X_i with the 2DEG, while its second term compensates for the dephasing of P_i^L and ensures the orthogonality $\langle X_i|\overline{\psi}_1\rangle = 0$.

We can perform a similar analysis of the time-evolved $2-h$ state by separating out in Eq. (17) the contribution of the noninteracting two-exciton states $|X_iX_{i'}\rangle$.[12,37] This contribution describes the time evolution of the two X's photoexcited by the optical field in the absence of interactions. However, the two X's interact with each other as well as with the 2DEG, as described by the equation

$$H|X_iX_{i'}\rangle = (\Omega_i+\Omega_{i'})|X_iX_{i'}\rangle - \sum_{j\neq i'} V_{ji'}|X_iX_j\rangle - \sum_{j\neq i} V_{ji}|X_jX_{i'}\rangle + |X_iY_{i'}\rangle + |X_{i'}Y_i\rangle + |B_{ii'}\rangle, \quad (26)$$

obtained by using Eq. (22) to calculate the state $[H,\hat{X}_i^\dagger\hat{X}_{i'}^\dagger]|0\rangle$. The first term in Eq. (26) is the energy of the two noninteracting X's, while the next two terms come from the Coulomb-induced LL coupling. Similar to $|X_iX_{i'}\rangle$, the state $|X_iY_{i'}\rangle = \hat{X}_i^\dagger\hat{Y}_{i'}^\dagger|0\rangle$ describes a noninteracting pair of X_i and $Y_{i'}$ excitations. Finally, as for the undoped case, the last term in Eq. (26),

$$|B_{ii'}\rangle = [\hat{Y}_i^\dagger,\hat{X}_{i'}^\dagger]|0\rangle = [[H,\hat{X}_i^\dagger],\hat{X}_{i'}^\dagger]|0\rangle, \quad (27)$$

comes from the X-X interactions.[12,37] Equation (B1) demonstrates that the state $|B_{ii'}\rangle$ is a linear combination of two e-h pairs with different center-of-mass momenta, but with the 2DEG in its ground-state, and thus describes biexciton bound, X_2, and scattering, XX, states similar to the undoped system.[12,37]

The X-X and X-2DEG interactions contribute to the time evolution of the photoexcited 2-h state in Eq. (17) through $|\psi_2^{int}\rangle$. We further decompose the latter state into (a) the contribution of the noninteracting pair of X_j-$|\overline{\psi}_1\rangle$ $1h$ excitations, and (b) the contribution $|\overline{\psi}_2\rangle$ due to the interactions between all the different pairs of 1-h excitations, i.e., the X-X interactions (as in the undoped system) and the X interactions with the $\{1-h/\text{2DEG}^*\}$ states (such as the four-particle Y excitations discussed above).

To obtain the equation of motion of the correlated 2-h contribution $|\overline{\psi}_2\rangle$, we note that the time-evolved state $|\psi_2\rangle$ contributes to the third-order nonlinear response at second order in the applied field. By taking the time derivative of Eq. (17) and using Eqs. (13), (22), (23), (25), and (26), we obtain that

$$i\partial_t|\bar{\psi}_2\rangle - H|\bar{\psi}_2\rangle = \frac{1}{2}\sum_{ii'} P_i^L P_{i'}^L |B_{ii'}\rangle + \sum_i [P_i^L \hat{Y}_i^\dagger - \bar{P}_i^L \hat{X}_i^\dagger]|\bar{\psi}_1\rangle. \quad (28)$$

Recalling that $|B_{ii'}\rangle$, Eq. (27), is the interacting two-exciton state, we see that the first term on the right-hand side (rhs) of the above equation describes the X-X interaction effects similar to the undoped case.[12,36–38,40] The second term describes the scattering of X_i with the carriers in the $\{1-h/2\text{DEG}^*\}$ state $|\bar{\psi}_1\rangle$.

Finally, we turn to the $0-h$ state. In Eq. (18) we split this state into the contribution of the ground state $|0\rangle$, with amplitude $\langle 0|\psi\rangle = \langle 0|\psi_0\rangle$, and the $\{0-h/2\text{DEG}^*\}$ contribution $|\psi_0^{int}\rangle$. The latter 2DEG* contribution is generated by the two-photon processes of excitation and deexcitation of the system accompanied by the scattering of 2DEG excitations, and is further decomposed into two parts. The first part, $-\Sigma_i P_i^{L*}\hat{X}_i|\bar{\psi}_1\rangle$, describes the de-excitation (after time t), of X_i from the $\{1-h/2\text{DEG}^*\}$ state $|\bar{\psi}_1\rangle$ without scattering with the $|\bar{\psi}_1\rangle$ carriers. The latter scattering, as well as the time evolution of the 2DEG excitations created via second-order processes analogous to the ones that lead to the inelastic Raman scattering signal,[41] are described by the second part, $|\bar{\psi}_0\rangle$.

The $0-h$ state $|\psi_0\rangle$ contributes to the third-order nonlinear response to second order in the optical field. By substituting Eq. (18) into Eq. (11) and using Eqs. (22)–(25), we obtain the equation of motion

$$i\partial_t|\bar{\psi}_0\rangle - H|\bar{\psi}_0\rangle = \sum_{ii'} P_i^{L*} P_{i'}^L \hat{X}_i|Y_{i'}\rangle + \sum_i [P_i^{L*}\hat{Y}_i - \bar{P}_i^{L*}\hat{X}_i]|\bar{\psi}_1\rangle - \sum_{ii'} P_i^{L*}\bar{P}_{i'}^L \hat{X}_i|X_{i'}\rangle - \mu\mathcal{E}^*\sum_{ii'} N_i^{1/2} P_{i'}^L([\hat{X}_i,\hat{X}_{i'}^\dagger] - \delta_{ii'})|0\rangle. \quad (29)$$

The first term in Eq. (29) describes the photoexcitation of the 2DEG via the second-order process where the exciton $X_{i'}$, photoexcited with amplitude $P_{i'}^L$, scatters with the 2DEG into the state $|Y_{i'}\rangle$, and then the exciton X_i is deexcited with amplitude P_i^L. The above process leaves the system in a 2DEG* state. It is analogous to the photoexcitation of coherent phonons in undoped semiconductors, and dominates the inelastic Raman-scattering spectra of the 2DEG.[41] The second term on the rhs of Eq. (29) describes the scattering of X_i with the carriers in $|\bar{\psi}_1\rangle$ during its deexcitation. The rest of the terms describe the possibility to create 2DEG excitations by photoexciting an exciton whose hole then recombines with a 2DEG electron.

IV. NONLINEAR POLARIZATION EQUATION OF MOTION

In this section we derive the equation of motion of the third-order nonlinear polarization $P_i(t)$ that determines the FWM and pump-probe nonlinear optical signal, and separate out the factorizable from the correlated contributions. When we discuss the physical meaning of the different terms, we focus on the FWM.

By taking the time derivative of Eq. (9) and using the definition of the operator $\hat{Y}_i$, Eq. (22), we obtain that

$$i\partial_t P_i(t) - \Omega_i P_i(t) + \sum_{i'\neq i} V_{ii'} P_{i'}(t) = -\mu\mathcal{E}(t)\sum_{i'} N_{i'}^{1/2}\langle\psi|[\hat{X}_i,\hat{X}_{i'}^\dagger]|\psi\rangle + \langle\psi|\hat{Y}_i|\psi\rangle. \quad (30)$$

The first term on the rhs of the above equation describes the Pauli blocking effects that only lead to positive time delay FWM signal and are determined by the density of the LLi photoexcited carriers [recall Eqs. (6) and (7)]. The second term describes the optical signal generated by the interactions between the recombining exciton X_i leading to the coherent emission and the photoexcited and 2DEG carriers. This interaction contribution dominates the FWM signal for negative time delays.[1] The above two source terms can be obtained by considering their equations of motion, which leads to an infinite hierarchy of equations of motion. Alternatively, one can first separate out the 2DEG* and the X-X and X-$|\bar{\psi}_1\rangle$ interaction contributions by using the decompositions of the photoexcited state, Eqs. (15), (17), and (18), and by retaining contributions up to third order in the optical field. Using the property $\langle 0|\hat{X}_{i'}\hat{Y}_i = \langle 0|\hat{Y}_i\hat{X}_{i'} + \langle 0|B_{ii'}$ [Eq. (27)], the expansion Eq. (10), and some algebra, we then obtain that

$$\langle\psi|\hat{Y}_i|\psi\rangle = \sum_{i'} P_{i'}^{L*}\langle B_{ii'}|\psi_2\rangle + \sum_{i'} P_{i'}^L\langle M_{ii'}|\bar{\psi}_0\rangle^* + \frac{1}{2}\sum_{i'j'} P_{i'}^L P_{j'}^L\langle\bar{\psi}_1|[[\hat{Y}_i,\hat{X}_{i'}^\dagger],\hat{X}_{j'}^\dagger]|0\rangle + \sum_{i'} P_{i'}^L\langle\bar{\psi}_1|[\hat{Y}_i,\hat{X}_{i'}^\dagger]|\bar{\psi}_1\rangle + \bar{P}_i, \quad (31)$$

where we introduced the state

$$|M_{ii'}\rangle = \hat{Y}_i|X_{i'}\rangle. \quad (32)$$

Noting that $\langle 0|M_{ii'}\rangle = 0$, we see that the above state describes an excited 2DEG configuration with full valence band. The first term in Eq. (31) describes the X-X interactions. Its equation of motion can be obtained by projecting the state $\langle B_{ii'}|$ to Eq. (13). In many cases, it is useful to decompose the above contribution into HF and correlated X-X interaction contributions by using Eq. (17):

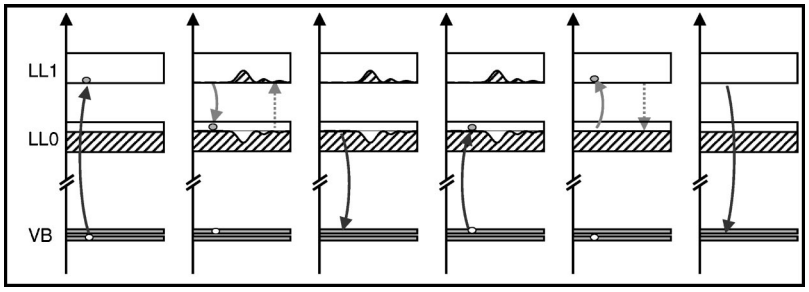

FIG. 3. Dominant resonant process determining the MP correlation contribution to the FWM signal. The first three panels show the Stokes-Raman scattering that creates the MP, while the other three panels show the reverse process that returns the system to the ground state.

$$\langle B_{ii'}|\psi_2\rangle=\frac{1}{2}\sum_{j'j}\langle B_{ii'}|X_jX_{j'}\rangle P_j^L P_{j'}^L + \sum_j P_j^L\langle B_{ii'}|X_j^\dagger|\bar{\psi}_1\rangle+\mathcal{B}_{ii'}. \quad (33)$$

The first term describes the HF X-X interactions, similar from the undoped case.[12] The second term comes from the exchange process where the first optical transition creates the state $|\bar{\psi}_1\rangle$ and the second transition excites an X_j e-h pair while returning the conduction electrons to their ground state. The above process results in two e-h pairs that scatter each other while the 2DEG is at rest. Subsequently, one of the above pairs, i', is deexcited by the optical field, while the remaining pair, i, recombines and leads to the coherent emission. The last term in Eq. (33) describes biexciton and X-X scattering correlations. Similar to the undoped case,[12,37] such effects are characterized by the amplitude of the correlated $2-h$ photoexcited state,

$$\mathcal{B}_{ii'}(t)=\langle B_{ii'}|\bar{\psi}_2\rangle. \quad (34)$$

The effects due to the propagation in time of the intermediate 2DEG excitations, photoexcited via the two-photon process in Fig. 1(a), are described by the amplitude

$$\mathcal{M}_{ii'}(t)=\langle M_{ii'}|\bar{\psi}_0\rangle. \quad (35)$$

Such time propagation leads to non-Markovian effects. In the case of particular interest here, the corresponding resonant contribution to the FWM signal is due to the nonlinear optical process shown in Fig. 3. The X photoexcited by the first optical transition decays into Y excitation. The e-h pair in this X-MP state then recombines, leading to coherent emission, and leaves the system in a MP state. This MP propagates in time and then scatters with the second photoexcited X into an X state subsequently annihilated by the optical field. It is interesting to note the similarity of this process and the familiar one of coherent anti-Stokes Raman scattering[42] that, however, involves phonons.

The second line in Eq. (31) describes a shakeup of the 2DEG during the exciton recombination that gives the coherent emission. In particular, the photoexcitation of two excitons, $X_{i'}$ and $X_{j'}$, is followed by the recombination of one of them assisted by the shakeup of a 2DEG excitation. The above process leaves the system in a $\{1-h/2\text{DEG}^*\}$ state, which is then annihilated by the optical field. To interpret the first term on the third line of Eq. (31), we note that the HF X-X interaction can be thought of as arising from the scattering of the polarization with the coherent density.[43] Similarly, this term describes the scattering of the polarization with the incoherent density of photoexcited carriers in the $\{1-h/2\text{DEG}^*\}$ state $|\bar{\psi}_1\rangle$.

Finally, the last term on the rhs of Eq. (31) is the correlated contribution

$$\bar{P}_i=\langle\psi_0|0\rangle\langle Y_i|\psi_1\rangle+\sum_j P_j^{L*}\langle Y_iX_j|\psi_2\rangle + \langle\bar{\psi}_0|\hat{Y}_i|\bar{\psi}_1\rangle+\langle\bar{\psi}_1|\hat{Y}_i|\bar{\psi}_2\rangle. \quad (36)$$

The first two terms of Eq. (36) describe the dephasing of the X and 2-X amplitudes that determine the third-order nonlinear polarization, while the last two terms describe the dephasing of the incoherent contribution to the nonlinear polarization. Note that, by linearizing the above equation, we recover the correlation function $\bar{P}_i^L$ [Eq. (24)] that describes the dephasing of the linear polarization P_i^L.

Using the above results we obtain the following equation of motion for the third-order nonlinear polarization:

$$\begin{aligned} i\partial_t P_i-\Omega_iP_i+\sum_{i'\neq i}V_{ii'}P_{i'}-\bar{P}_i &= \mu\mathcal{E}\sum_{i'}N_{i'}^{1/2}\langle\psi_1|(\delta_{ii'}-[\hat{X}_i,\hat{X}_{i'}^\dagger])|\psi_1\rangle \\ &+\frac{1}{2}\sum_{jj'i'}\langle B_{ij}|X_{i'}X_{j'}\rangle P_{i'}^L\,P_{j'}^L P_j^{L*}+\sum_{i'}\mathcal{B}_{ii'}P_{i'}^{L*} \\ &+\sum_{i'}P_{i'}^L\mathcal{M}_{ii'}^*+\frac{1}{2}\sum_{i'j'}P_{i'}^L\,P_{j'}^L\langle 0|[\hat{X}_{j'},[\hat{X}_{i'},\hat{Y}_i^\dagger]]|\bar{\psi}_1\rangle^* \\ &+\sum_{i'}P_{i'}^L\langle\bar{\psi}_1|[\hat{Y}_i,\hat{X}_{i'}^\dagger]|\bar{\psi}_1\rangle+\sum_{ji'}P_{i'}^LP_j^{L*}\langle B_{ij}|X_{i'}^\dagger|\bar{\psi}_1\rangle. \end{aligned} \quad (37)$$

In the above equation we have separated out the source terms into (i) a coherent part, determined by Pauli blocking effects, HF X-X interactions, and the propagation in time of the intermediate interacting X-X and 2DEG^* states (first four terms on the rhs), and (ii) an incoherent part, determined by the $\{1-h/2\text{DEG}^*\}$ photoexcited state $|\bar{\psi}_1\rangle$ (last three terms on the rhs) and the correlated nonlinear contribution $\bar{P}_i$. It is worth noting in the above equation that the terms propor-

tional to the polarization $P^L_{i'}$ describe a time-dependent photoinduced renormalization of the X_i energy and dephasing $(i'=i)$, and of the coupling $V_{ii'}$ of the X_i and $X_{i'}$ states $(i'\neq i)$. If the $\{1-h/2\text{DEG}^*\}$ and $|B_{ii'}\rangle$ excitations decay rapidly, while the 2DEG excitations are long lived, then the non-Markovian LL coupling and dephasing effects are dominated by the correlation function $\mathcal{M}_{ii'}(t)$.

As demonstrated by the above equation, the Coulomb correlations lead to new contributions to the nonlinear polarization, determined by many-particle correlation functions. In the following section, we turn to the problem of solving for the correlation functions on the rhs of Eq. (37), and address the issue of dephasing in a strongly correlated electronic system.

V. DEPHASING AND CORRELATION PROCESSES

The equations of motion for the correlation functions that enter in Eq. (37) may be obtained after introducing a basis suitable for describing the $1h$, $2h$, and $0h$ states. In strongly correlated systems, an expansion in terms of the pair excitations of a noninteracting many electron may not be convenient. In general, we must introduce a basis of strongly correlated states that already incorporate the ground-state correlations. The choice of such a basis depends on the ground-state and on the most important excitations for the experimental parameters of interest (e.g., the filling factor, the central excitation frequency, the polarization of the optical field, etc).

Our goal in the rest of this paper is to identify the dominant features in the FWM spectrum at the magnetoexciton energies that come from the interactions and time propagation of the MP collective modes. Analogous questions regarding the role of X-X interactions in undoped semiconductors were first addressed by using average polarization models.[2,15] As we show in the following section, a generalized average polarization model can be extracted from the theory developed in the previous sections after introducing a basis of Lanczos strongly correlated states.[35] This model explains the main qualitative features observed in recent FWM experiments.[30]

We start by considering a basis for the 1-h state $|\overline{\psi}_1\rangle$. Noting the analogy with X-phonon interactions in the undoped system discussed in the Introduction, we would like to consider a basis that consists of products of e-h pair and MP wave functions. In the undoped system, such states have the form $\hat{e}^\dagger_{\mathbf{k}-\mathbf{q}}\hat{h}^\dagger_{\mathbf{k}}a^\dagger_{\mathbf{q}}|0\rangle$, where $a^\dagger_{\mathbf{q}}$ creates the phonon state, $\hat{e}^\dagger_{\mathbf{k}-\mathbf{q}}\hat{h}^\dagger_{\mathbf{k}}$ creates the two-particle e-h pair wave function, and $|0\rangle$ is annihilated by all the $\hat{e}$ and $\hat{h}$ operators.[8,11,39] In our case, however, the ground state $|0\rangle$ may contain a strongly correlated electron gas, while, unlike for phonons, the MP creation operators are made of electrons. Thus we must use a basis of strongly correlated states, which is made out of electrons.

A basis set useful for calculating the Green's functions for tight binding and Hubbard Hamiltonians is the Lanczos basis.[35] Such correlated states can be used to obtain exact solutions in the case of small systems,[23] but also to approximately describe continuum resonances in large systems, e.g., the Fano resonances in the absorption spectrum of semiconductor superlattices.[44] Each new basis state is obtained by acting with the Hamiltonian H on the previous state, and then orthogonalizing the result with respect to all existing basis states.[35] This procedure is similar to Eq. (19) that introduced the states $|Y_i\rangle$, and led us to the parameters Ω_i and $V_{ii'}$, Eqs. (20) and (21). A new basis state $|Z_i\rangle=\hat{Z}^\dagger_i|0\rangle$ is now constructed from the relation

$$H|Y_i\rangle=\overline{\Omega}_i|Y_i\rangle+\sum_{i'} W_{i'i}|X_{i'}\rangle+|Z_i\rangle, \tag{38}$$

where

$$\overline{\Omega}_i=\frac{\langle Y_i|H|Y_i\rangle}{\langle Y_i|Y_i\rangle} \tag{39}$$

is the average energy of the four-particle excitation $|Y_i\rangle$,

$$W_{i'i}=\langle X_{i'}|H|Y_i\rangle \tag{40}$$

gives the probability amplitude that Y_i scatters into $X_{i'}$, and we introduced the operator

$$\hat{Z}_i=[\hat{Y}_i,H]-\overline{\Omega}_i\hat{Y}_i-\sum_{i'} W_{ii'}\hat{X}_{i'}. \tag{41}$$

Using Eqs. (38)–(40), as well as the orthogonality $\langle X_j|Y_i\rangle=0$, one can see that the state $|Z_i\rangle$ is orthogonal to all the states $|X_j\rangle$, $j=0,1,\ldots$, and to $|Y_i\rangle$. Therefore, it is a linear combination of all the 2DEG* states into which $|Y_i\rangle$ can scatter. Additional basis states can be constructed by applying the above orthogonalization procedure to the state $H|Z_i\rangle$. We note here that the states $|X_j\rangle$, $|Y_i\rangle$, $|Z_i\rangle$, ... do not correspond to an expansion in terms of excitations of a noninteracting many-electron state, since they are obtained by the action of the operators $\hat{X}^\dagger_j$, $\hat{Y}^\dagger_i$, $\hat{Z}^\dagger_i$, ... on the ground eigenstate $|0\rangle$ of the many-body Hamiltonian H.

By using Eq. (19) and the orthogonality $\langle X_j|Y_i\rangle=0$, we obtain the useful relation

$$W_{i'i}=\langle Y_{i'}|Y_i\rangle=W^*_{ii'}. \tag{42}$$

Note that $\langle Y_{i'}|Y_i\rangle\neq 0$, and we may also have that $\langle Y_{i'}|Z_i\rangle\neq 0$ for $i'\neq i$. If this is the case we need to orthogonalize the independent states $|Y_{i'}\rangle$, and then subtract a linear combination of the latter from $|Z_i\rangle$ in Eq. (38), so that all the Z and Y states become orthogonal. However, in the electron-hole symmetric limit of the 2DEG system, $|Y_i\rangle$ is the same state for all i when only LL0 and LL1 contribute (see Appendix A), and thus the latter procedure is not needed.

Equations of motion for all correlation functions determined by the state $|\overline{\psi}_1\rangle$ can be obtained after expanding in a basis set of $\{1-h/2\text{DEG}^*\}$ states. Let us consider, for example, $\overline{P}^L_i(t)$ [Eq. (24)], which describes the dephasing of the linear polarization $P^L_i(t)$. If we choose the Lanczos basis discussed above, we obtain [after multiplying Eq. (25) by $\langle Y_i|$ and using Eqs. (38)–(40)] the equation of motion

$$i\partial_t \overline{P}_i^L = \overline{\Omega}_i \overline{P}_i^L + \sum_{i'} W_{ii'} P_{i'}^L + \mathcal{Z}_i^L, \tag{43}$$

where we introduced the correlation function $\mathcal{Z}_i^L = \langle Z_i | \overline{\psi}_1 \rangle$ whose equation of motion can be obtained in a similar way as that of $\overline{P}_i^L$.

It is important to note that the dephasing of the optical polarization obtained as above is non-Markovian. Indeed, after solving Eqs. (23) and (43) by Fourier transform, we obtain that

$$[\omega - \Omega_i(\omega)] P_i^L(\omega) + \sum_{i' \neq i} V_{ii'}(\omega) P_{i'}^L(\omega) = -\mu \mathcal{E}(\omega) N_i^{1/2} + \frac{\mathcal{Z}_i^L(\omega)}{\omega - \overline{\Omega}_i}, \tag{44}$$

where the X energy $\Omega_i(\omega)$ and the coupling between the X states $V_{ii'}(\omega)$ include frequency-dependent self-energy corrections due to the X-2DEG scattering,

$$\Omega_i(\omega) = \Omega_i + \frac{W_{ii}}{\omega - \overline{\Omega}_i}, \quad V_{ii'}(\omega) = V_{ii'} + \frac{W_{ii'}}{\omega - \overline{\Omega}_i}. \tag{45}$$

Additional self-energy corrections arise from $\mathcal{Z}^L$, discussed in the following section. The frequency dependence of the above X energies and coupling constants is a manifestation of the non-Markovian behavior of the system. This arises because part of the optical excitation is temporarily stored in the shake-up excitations described by $\overline{P}_i^L$.

Using the recursive method we can also construct a basis for the 2-h and 0-h states, which we can then use to calculate the correlation functions determined by the states $|\overline{\psi}_2\rangle$ and $|\overline{\psi}_0\rangle$. We start with the 2-$h$ state $|B_{ii'}\rangle$ that determines the X-X correlation function $\mathcal{B}_{ii'}$, and introduce the Lanczos state $|\overline{B}_{ii'}\rangle$ as follows:

$$H|B_{ii'}\rangle = \Omega_{ii'}^B |\mathcal{B}_{ii'}\rangle + |\overline{B}_{ii'}\rangle, \quad \Omega_{ii'}^B = \frac{\langle B_{ii'}|H|B_{ii'}\rangle}{\langle B_{ii'}|B_{ii'}\rangle}, \tag{46}$$

where $\Omega_{ii'}^B$ is the average energy of the interacting 2-X state $|B_{ii'}\rangle$. The state $|\overline{B}_{ii'}\rangle$, $\langle \overline{B}_{ii'}|B_{ii'}\rangle = 0$, is a linear combination of all the 2-X states into which $|B_{ii'}\rangle$ can scatter. By projecting the state $\langle B_{ii'}|$ to Eq. (28) and using Eq. (46), we then obtain from Eq. (34) the equation of motion

$$i\partial_t \mathcal{B}_{ii'} - \Omega_{ii'}^B \mathcal{B}_{ii'} = \frac{1}{2} \sum_{j'j} \langle B_{ii'}|B_{jj'}\rangle P_{j'}^L P_j^L + \sum_j P_j^L \langle B_{ii'}|\hat{Y}_j^\dagger|\overline{\psi}_1\rangle - \sum_j \overline{P}_j^L \langle B_{ii'}|\hat{X}_j^\dagger|\overline{\psi}_1\rangle + \overline{\mathcal{B}}_{ii'}, \tag{47}$$

where $\overline{\mathcal{B}}_{ii'}(t) = \langle \overline{B}_{ii'}|\overline{\psi}_2\rangle$. The above equation describes the time evolution of the "intermediate" 2-X state $|B_{ii'}\rangle$, which is created by the X-X interactions. In the case of undoped QW magnetoexcitons, $\mathcal{B}_{ii'}(t)$ corresponds to $F(t)$ of Ref. 37.

One should note here the similarity of Eq. (47) and the average polarization model that has been successful in describing the X-X correlations and biexciton effects in undoped semiconductors.[2,15,37] This model includes the X-X self-energy effects due to the higher Lanczos states $|\overline{B}_{ii'}\rangle, \ldots$ via a phenomenological dephasing rate. The validity of such a model in the case of undoped QW magnetoexcitons was analyzed in Ref. 37.

Similar to $\mathcal{B}_{ii'}$, the correlation function $\mathcal{M}_{ii'}$ describes the time evolution of the "intermediate" photoexcited 2DEG* state $|M_{ii'}\rangle$. Using the Lanczos method we obtain that

$$H|M_{ii'}\rangle = \Omega_{ii'}^M |M_{ii'}\rangle + |\overline{M}_{ii'}\rangle, \quad \Omega_{ii'}^M = \frac{\langle M_{ii'}|H|M_{ii'}\rangle}{\langle M_{ii'}|M_{ii'}\rangle}, \tag{48}$$

where $\Omega_{ii'}^M$ is the average MP energy, and the state $|\overline{M}_{ii'}\rangle$, $\langle \overline{M}_{ii'}|M_{ii'}\rangle = 0$, is a linear combination of all the states into which $|M_{ii'}\rangle$ can scatter. We then obtain, after projecting $\langle M_{ii'}|$ on Eq. (29), the equation of motion

$$\begin{aligned} i\partial_t \mathcal{M}_{ii'} - \Omega_{ii'}^M \mathcal{M}_{ii'} - \overline{\mathcal{M}}_{ii'} &= \sum_{jj'} \langle M_{ii'}|\hat{X}_j|Y_{j'}\rangle P_j^{L*} P_{j'}^L + \sum_j P_j^{L*} \Big[\langle M_{ii'}|\hat{Y}_j|\overline{\psi}_1\rangle \\ &\quad - \sum_{j'} \langle M_{ii'}|\hat{X}_j|X_{j'}\rangle \overline{P}_{j'}^L \Big] - \sum_j \overline{P}_j^{L*} \langle M_{ii'}|\hat{X}_j|\overline{\psi}_1\rangle \\ &\quad + \mu \mathcal{E}^* \sum_{j'j} N_j^{1/2} P_{j'}^L \langle M_{ii'}|(\delta_{jj'} - [\hat{X}_j, \hat{X}_{j'}^\dagger])|0\rangle, \end{aligned} \tag{49}$$

where $\overline{\mathcal{M}}_{ii'} = \langle \overline{M}_{ii'}|\overline{\psi}_0\rangle$ describes the dephasing of $\mathcal{M}_{ii'}$. In the case of the 2DEG, the single-mode approximation[23] suggests that the latter dephasing can be treated to first approximation by introducing a phenomenological dephasing rate.

The remaining step is the calculation of the correlated contribution $\overline{P}_i$, Eq. (36). The equation of motion for the first two terms of Eq. (36) can be easily obtained from Eqs. (12) and (13) after using Eq. (38) and the property

$$\langle Y_i X_j|H = (\overline{\Omega}_i + \Omega_j)\langle Y_i X_j| - \sum_{j' \neq j} V_{jj'} \langle Y_i X_{j'}| + \sum_{i'} W_{ii'} \langle X_{i'} X_j| + \langle Y_i|\hat{Y}_j + \langle Z_i|\hat{X}_j, \tag{50}$$

obtained by calculating the commutator $[\hat{Y}_i \hat{X}_j, H]$ using Eqs. (22) and (38). The equations of motion for the last two terms in Eq. (36) can be obtained from Eqs. (29), (25), and (28) by using Eq. (41) and the basis of choice. We thus obtain the equation of motion

$$i\partial_t \overline{P}_i - \overline{\Omega}_i \overline{P}_i - \mathcal{Z}_i = \sum_{i'} W_{ii'} P_{i'} + \mathcal{Q}_{Y_i}, \tag{51}$$

where the correlated contribution

$$\mathcal{Z}_i = \langle \psi_0|0\rangle\langle Z_i|\psi_1\rangle + \sum_j P_j^{L*}\langle Z_i|\hat{X}_j|\psi_2\rangle + \langle \overline{\psi}_0|\hat{Z}_i|\overline{\psi}_1\rangle + \langle \overline{\psi}_1|\hat{Z}_i|\overline{\psi}_2\rangle \tag{52}$$

has the same structure as $\overline{P}_i$ (with the difference $\hat{Y}_i \to \hat{Z}_i$) and describes the dephasing of $\overline{P}_i$. The factorizable contribution $\mathcal{Q}_{Y_i}$ describes photoinduced nonlinear corrections to the dephasing and energy of $\overline{P}_i$, and to the scattering amplitudes $W_{ii'}$. The equation of motion for $\mathcal{Z}_i$, which to first order in the optical field coincides with $\mathcal{Z}_i^L$, has a form analogous to that of $\overline{P}_i$.

One should note here that the correlation function $\overline{P}_i$ can be decomposed further in the case of systems where the X-X interaction contribution to the operator $\hat{Y}_i$ can be separated out. This is possible, for example, in undoped semiconductors,[8,11] where the operator $\hat{Y}_i$ can be decomposed into a part that is independent of the phonon variables, which describes the X-X Coulomb interactions, and a part that describes the phonon creation/annihilation processes. The former X-X contribution comes from the last term in Eq. (36); and corresponds to the correlation function $\overline{Z}$ of Refs. 8 and 11, which mainly contributes to the six-wave-mixing spectra.[45] The above distinction between the interaction processes is possible in systems where the creation operators of the ground-state excitations of interest (phonons, MP's, magnons, . . .) commute with the electronic operators that describe the photoexcited carriers.

VI. GENERALIZED AVERAGE POLARIZATION MODEL

In this section we present an example of how the theoretical framework developed so far can be used to describe the nonlinear optical dynamics of the 2DEG in a high magnetic field. We consider the case where only the first two LL's are photoexcited, so we retain in our calculations only the LL0 and LL1 magnetoexcitons. We focus on filling factors close to $\nu=1$, where the ground-state 2DEG populates spin-$\uparrow$ LL0 states,[32,33] and on photoexcitation with σ_+ circularly polarized light, which excites spin-$\downarrow$ electrons.[30] The above conditions apply to the experiment of Ref. 30, which we wish to interpret.

The electron-hole symmetry of the ideal 2D system, analyzed in Appendix A, relates the correlation functions and interaction parameters with different LL indices that enter in the equations of motion. For example, in Appendix A we derive the symmetry property

$$\sqrt{1-\nu_1}\hat{Y}_1 = -\sqrt{1-\nu_0}\hat{Y}_0 = \hat{Y}, \tag{53}$$

where $\hat{Y}$ is determined by Eq. (A17). The above symmetry relation can be used to reduce the number of independent variables. For example, from Eqs. (39), (42), and (36) we obtain $\overline{\Omega}_i = \overline{\Omega}$, $W_{10} = W_{01}$,

$$(1-\nu_i)W_{ii} = -\sqrt{(1-\nu_0)(1-\nu_1)}W_{01} = W = \langle Y|Y\rangle, \tag{54}$$

$$\sqrt{1-\nu_1}\overline{P}_1(t) = -\sqrt{1-\nu_0}\overline{P}_0(t) = W\overline{P}(t), \tag{55}$$

where $i=0,1$. It is then convenient to make the transformation

$$P_i \to P_i\sqrt{1-\nu_i}, \tag{56}$$

and redefine for simplicity

$$V_{ii'} \to V_{ii'}\sqrt{(1-\nu_i)(1-\nu_{i'})}, W \to W(1-\nu_0)(1-\nu_1). \tag{57}$$

Using the above relations we obtain from Eq. (23) the following equations of motion for the linear polarizations:

$$i\partial_t P_0^L = (\Omega_0 - i\Gamma_0)P_0^L - [\mu\mathcal{E}(t) + V_{01}(1-\nu_1)P_1^L + W(1-\nu_1)\overline{P}^L], \tag{58}$$

$$i\partial_t P_1^L = (\Omega_1 - i\Gamma_1)P_1^L - [\mu\mathcal{E}(t) + V_{10}(1-\nu_0)P_0^L - W(1-\nu_0)\overline{P}^L]. \tag{59}$$

The above equations have the form of two coupled two-level systems, corresponding to the LL0 and LL1 magnetoexcitons. This form is due to the zero-dimensional confinement induced by the QW potential and the magnetic field, which leads to the novel 2DEG properties.[23,24] The Coulomb interactions renormalize the Rabi energy $\mu\mathcal{E}$ by a mean- (local-) field correction proportional to the polarization (analogous to the undoped system,[43]) and by a 2DEG shake-up correction proportional to $\overline{P}^L$.

As demonstrated by Eqs. (58) and (59), the polarization dephasing is determined, in addition to the phonon-induced dephasing rates Γ_i, by the correlation function $\overline{P}^L$. For weak Γ_i, $\overline{P}^L$ dominates. In the absence of magnetic field, $\overline{P}^L$ describes the shakeup of FS pair excitations, and leads to a non-Markovian dephasing due to the nonperturbative h-FS interactions.[9,17] For the experimental conditions of interest here, $\overline{P}^L$ originates primarily from the X scattering to the continuum of X-MP states composed of an X and a MP with opposite momenta. An analogy can be drawn between the above X-MP states and the continuum of X-X scattering states in undoped semiconductors.[1,2,37]

We now turn to the dephasing of the X-MP correlation function $\overline{P}^L$. This X-MP dephasing originates from the Coulomb-induced coupling of the Lanczos states $|Y\rangle, |Z\rangle, |Z'\rangle, \ldots$. We note that $\mathcal{Z}^L$ and higher correlation functions do not couple to P^L, but only to the amplitudes corresponding to the previous and the next Lanczos states. For example, the equation of motion for $\mathcal{Z}^L$ reads

$$i\partial_t \mathcal{Z}^L = \bar{\Omega}_Z \mathcal{Z}^L + W_{ZY}\bar{P}^L + \langle Z'|\bar{\psi}_1\rangle, \tag{60}$$

where we defined

$$\bar{\Omega}_Z = \frac{\langle Z|H|Z\rangle}{\langle Z|Z\rangle}, \quad W_{ZY} = \frac{\langle Z|Z\rangle}{\langle Y|Y\rangle} = \frac{\langle Z|H|Y\rangle}{W}. \tag{61}$$

The amplitudes of the higher Lanczos states satisfy similar equations of motion. After taking the Fourier transform and using the above symmetry properties and some algebra, we obtain that

$$\bar{P}^L(\omega) = \frac{P_1^L(\omega) - P_0^L(\omega)}{\omega - \bar{\Omega} + i\gamma_Y - W_{ZY}\Sigma_Z(\omega)}, \tag{62}$$

where γ_Y is the dephasing rate. The dephasing of $\bar{P}^L$ is thus described by the self-energy Σ_Z,

$$\Sigma_Z(\omega) = \frac{1}{\omega - \bar{\Omega}_Z + i\gamma_Z - W_{Z'Z}\Sigma_{Z'}(\omega)}, \tag{63}$$

where $\Sigma_{Z'}$ is given by Eq. (63) with $Z' \to Z''$.

The above equation can be used to obtain a continued fraction expansion for the self-energy. In the case of an N-electron system, such an expansion terminates after N iterations. To obtain true dephasing for finite N, we must introduce the damping rates of the Lanczos states, due to the neglected degrees of freedom of the $N\to\infty$ system. The convergence of the above self-energy expansion becomes more rapid with increasing damping rates.[44] In the QHE literature, numerical calculations of the N-electron spectral functions have been extrapolated to the $N\to\infty$ limit.[23]

Equation (63) can be solved analytically when the dispersion in the energies and matrix elements of the higher Lanczos states is small as compared to the frequencies of interest, so that the self-energy is approximately the same for all the higher Lanczos states.[35] This may be the case, for example, if the momenta close to the magnetoroton minimum, $q\sim 1/l$, dominate.[41] In the case of QW magnetoexcitons in undoped semiconductors, the validity of such an approximation for the X-X self-energy was discussed in Ref. 37.

A microscopic determination of $\Sigma_Z(\omega)$ is beyond the scope of this paper. Here we describe the X-MP scattering in a way similar to the average polarization model description of the X-X scattering.[2] In particular, we assume that Σ_Z is a sufficiently smooth function of frequency in the range of interest, in which case its frequency dependence can be neglected to first approximation. In the case of 2D magnetoexcitons in undoped semiconductors, a similar approximation was shown to apply for strong X-X interactions.[37] We thus obtain the equation

$$i\partial_t \bar{P}^L = (\bar{\Omega} - i\gamma)\bar{P}^L + P_1^L - P_0^L, \tag{64}$$

where the values of the renormalized Y state energy

$$\bar{\Omega} = \frac{\langle Y|H|Y\rangle}{\langle Y|Y\rangle} + W_{ZY}\mathrm{Re}\Sigma_Z(\bar{\Omega}) \tag{65}$$

and dephasing rate

$$\gamma = \gamma_Y - W_{ZY}\mathrm{Im}\,\Sigma_Z(\bar{\Omega}) \tag{66}$$

are estimated here by fitting to the experimental linear absorption spectrum.[30] The above approximation works best for sufficiently large γ. Due to the contribution to the Y state of finite momentum MP's and e-h pairs, we expect that $\bar{\Omega} > \Omega_1$, where Ω_1 [Eq. (20)] is the energy of the zero-momentum LL1 magnetoexciton.[41]

We now turn to the nonlinear polarization, determined by the equation of motion, Eq. (37). First we consider the X-X interaction contribution, described by the second line on the rhs of Eq. (37). For strong damping of the $2X$ states $|B_{ii'}\rangle$, the non-Markovian X-X scattering effects are suppressed,[12,37] and we only retain the HF X-X interaction contribution [second term on the rhs of Eq. (37)]. The X-X potentials $\langle B_{ii'}|X_jX_{j'}\rangle$, with different LL indices i and i', are related to each other in the electron-hole symmetric limit due to the property

$$(1-\nu_i)|B_{ii}\rangle = -\sqrt{(1-\nu_0)(1-\nu_1)}|B_{10}\rangle, \tag{67}$$

where $i=0,1$, which follows from Eq. (B1). Using the above relation and Eq. (56), we express the HF X-X interaction contribution in the form

$$\sum_{jj'} \sqrt{(1-\nu_j)(1-\nu_{j'})}\langle B_{ii}|X_jX_{j'}\rangle P_j^L P_{j'}^L (P_i^{L*} - P_{i'}^{L*}), \tag{68}$$

where $i'\neq i$ and the potential $\langle B_{ii}|X_jX_{j'}\rangle$ is evaluated in Appendix B.

The time dependence of the incoherent source terms in the last two lines of Eq. (37) is determined by the $\{1-h/2\mathrm{DEG}^*\}$ state $|\bar{\psi}_1\rangle$. The corresponding correlation functions dephase rapidly in the case of strong X-MP damping; unlike, e.g., the correlation function $\mathcal{M}$ that describes the time propagation of the long-lived MP's. The same holds for the FWM contributions due to the photoinduced renormalizations of the X-MP correlation functions $\bar{P}$, $\mathcal{Z}$, ..., which are described by the source terms $\mathcal{Q}_Y$, $\mathcal{Q}_Z$, ... in Eq. (51). The latter lead to an incoherent FWM contribution at the X-MP energies, which is broadened by the bare dephasing of $\bar{P}$. Here we neglect such incoherent contributions to the FWM spectrum. Similarly we approximate the photoexcited carrier density that determines the Pauli blocking contribution [first term on the rhs of Eq. (37)] by the coherent exciton density, P^LP^{L*}, and neglect the incoherent density contribution determined by $|\bar{\psi}_1\rangle$.

The correlation function $\mathcal{M}_{ii'}$ describes the time evolution of the long-lived MP intermediate states. For σ_+ photoexcitation, the exciton operators create spin-$\downarrow$ electrons, and thus the operators $\hat{X}_i\hat{X}_j^\dagger$ do not excite the spin-$\uparrow$ 2DEG. We therefore have that

$$\langle 2\mathrm{DEG}^*|\hat{X}_i|X_j\rangle \sim 0 \tag{69}$$

for any excited 2DEG state. Equation (69) is exact for $\nu=1$. Using Eq. (53) and Appendix C, we then derive the symmetry relations $\Omega_{ii'}^M = \Omega_M$, $\mathcal{M}_{10} = \mathcal{M}_{01}$,

$$(1-\nu_i)(1-\nu_j)\langle M_{ii}|\hat{X}_j|Y_j\rangle$$
$$=-(1-\nu_i)\sqrt{(1-\nu_j)(1-\nu_{j'})}\langle M_{ii}|\hat{X}_j|Y_{j'}\rangle$$
$$=-(1-\nu_i)\sqrt{(1-\nu_j)(1-\nu_{j'})}\langle M_{ii}|\hat{X}_{j'}|Y_j\rangle=W_M, \quad (70)$$

$$(1-\nu_i)\mathcal{M}_{ii}=-\sqrt{(1-\nu_0)(1-\nu_1)}\mathcal{M}_{01}=W_M\mathcal{M}, \quad (71)$$

for any i and $j\neq j'$. Neglecting the incoherent X-MP contribution to the rhs of Eq. (49), determined by $|\overline{\psi}_1\rangle$, as compared to the first term, determined by the exciton polarizations, we obtain the equation of motion

$$i\partial_t\mathcal{M}=(\Omega^M-i\gamma_M)\mathcal{M}-P_1^LP_0^{L*}+P_0^LP_0^{L*}+P_1^LP_1^{L*}$$
$$-P_0^LP_1^{L*}, \quad (72)$$

where the weak MP damping, which to first approximation can be described by the dephasing rate γ_M,[25,46] enhances the non-Markovian dephasing effects.

We note here that, in the absence of disorder, only the zero-momentum MP state contributes to the nonlinear optical signal. As already seen in the inelastic Raman-scattering spectra, the disorder leads to the photoexcitation of a state $|M\rangle$ with strong contribution from the finite momentum MP's close to the magnetoroton energy.[25,41,46] The energy Ω_M is the average energy of the coupled MP states, and exceeds the cyclotron energy Ω_c^c that gives the zero-momentum MP energy.

Using the above results, and redefining for simplicity $W_M\rightarrow W_M(1-\nu_0)(1-\nu_1)$, we obtain from Eqs. (37) and (51) the following closed system of equations for the nonlinear polarizations:

$$i\partial_tP_0=(\Omega_0-i\Gamma_0)P_0-V_{01}(1-\nu_1)P_1^L+2\mu\mathcal{E}(t)P_0^{L*}P_0^L$$
$$+2V_{01}(1-\nu_1)P_1^LP_0^L(P_0^{L*}-P_1^{L*})$$
$$+W_M(1-\nu_1)\mathcal{M}^*(P_0^L-P_1^L)-W(1-\nu_1)\overline{P}, \quad (73)$$

$$i\partial_tP_1=(\Omega_1-i\Gamma_1)P_1-V_{10}(1-\nu_0)P_0^L+2\mu\mathcal{E}(t)P_1^{L*}P_1^L$$
$$-2V_{10}(1-\nu_0)P_1^LP_0^L(P_0^{L*}-P_1^{L*}) \quad (74)$$
$$-W_M(1-\nu_0)\mathcal{M}^*(P_0^L-P_1^L)+W(1-\nu_0)\overline{P},$$

$$i\partial_t\overline{P}=(\overline{\Omega}-i\gamma)\overline{P}+P_1-P_0. \quad (75)$$

The second lines in Eqs. (73) and (74) describe the Pauli blocking PSF effects and HF X-X interactions similar to the undoped system,[43] while the third lines describe the correlation effects due to the time propagation of the intermediate Y and MP states. The latter correlations lead to a time-dependent coupling of the LL0 and LL1 levels, as well as to non-Markovian dephasing.

The set of four equations, Eqs. (73), (74), (75), and (72), together with the linear polarization equations of motion, Eqs. (58), (59), and (64), constitute our model. To obtain the FWM spectrum, we assume a laser excitation of the form $\mathcal{E}(t)=e^{i\vec{k}_2\cdot\vec{r}}\mathcal{E}_p(t)+e^{i\vec{k}_1\cdot\vec{r}}\mathcal{E}_p(t+\Delta t)$, where $\mathcal{E}_p(t)$ is the Gaussian envelope of the pulses emitted by the laser. We then solve the above equations as a function of time t and time delay Δt between the two pulses, keeping only the terms leading to a nonlinear signal in the $2\vec{k}_2-\vec{k}_1$ direction, and perform a Fourier transform of the nonlinear polarization to get

$$P(\omega,\Delta t)=(1-\nu_0)P_0(\omega,\Delta t)+(1-\nu_1)P_1(\omega,\Delta t). \quad (76)$$

The FWM signal measured in the experiments is proportional to $|P(\Delta t,\omega)|^2$ and is calculated in the next section.

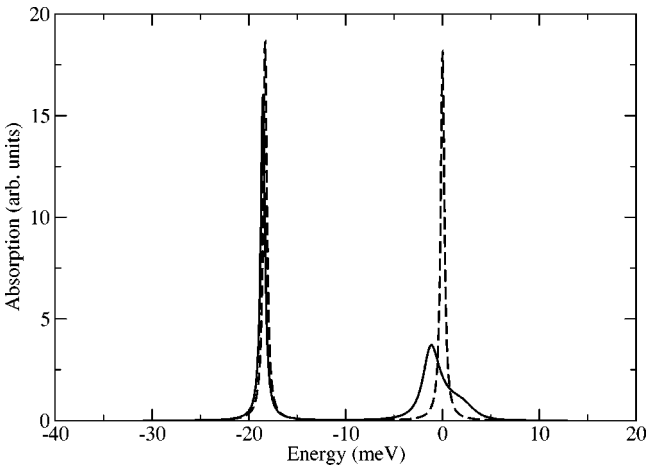

FIG. 4. Linear absorption spectrum (full line). The dashed line shows the spectrum for $\overline{P^L}=0$, in which case the dephasing is determined by the electron-phonon scattering. The interaction energies $\sqrt{W}=2.2$ meV and $V_{01}=0.5$ meV, the dephasing rates $\gamma\sim 3$ meV, and the X and Y energies were chosen to reproduce the linear absorption LL peak ratio, energy spacing, and line shape observed in the experiment of Ref. 30 for $B=8$ T and σ^+ circular polarization. In this case $\nu_0=0.075$ and $\nu_1=0$ (Ref. 30).

VII. NUMERICAL RESULTS

In this section we present the results of our numerical calculations, which are based on the model of Sec. VI. We start with the linear absorption spectrum, $\alpha(\omega)\propto\mathrm{Im}[P^L(\omega)/\mathcal{E}(\omega)]$. By fitting to the linear absorption measurements of Ref. 30, we can fix the interaction parameters V_{01} and W, the energies Ω_i and $\overline{\Omega}$, and the dephasing rates Γ_i and γ, to within $\pm 50\%$. Varying the parameters within this fitting range yields no significant change in the time and frequency dependence of the FWM or linear absorption spectrum. Figure 4 (full line) displays the two X peaks obtained in this way. Their broadening is determined by (a) the X-phonon scattering, described by dephasing rates $\Gamma_0\sim\Gamma_1$ similar to the undoped system, and (b) the X-2DEG scattering, described by the correlation function $\overline{P^L}$. The important role of the $X\rightarrow X$-MP scattering is clear by comparing with the dashed line curve of Fig. 4, obtained with $\overline{P^L}=0$. Although the X-2DEG scattering governs the line shape of the LL1 peak, it plays a very small role at the LL0 frequency. To

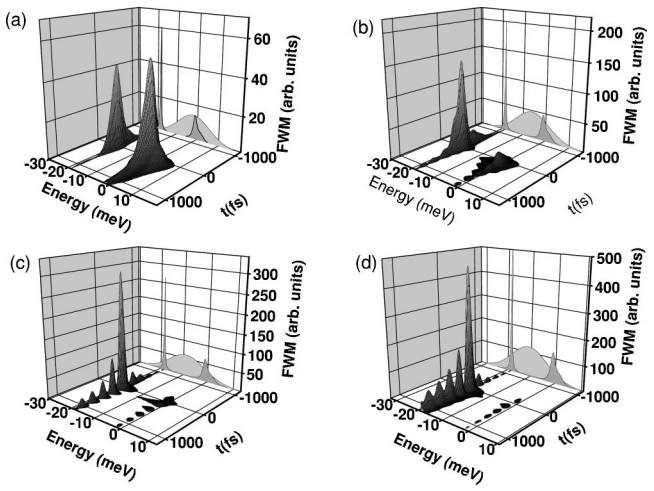

FIG. 5. Time delay and frequency dependence of the FWM spectrum for excitation frequency (a) at the LL1 peak, (b) shifted by 4 meV, (c) shifted by 7 meV, and (d) shifted by 9 meV. The optical pulse and linear absorption spectra are displayed in the back panel. The pulse duration was 150 fs, $\Omega_M = 17.5$ meV, $\sqrt{W_M} = 2$ meV, and $\gamma_M = 0.2$ meV.

interpret this behavior, we note that the main contribution to $\overline{P^L}$ comes from $\{1\text{-MP}+1\text{-LL0-}e+1\text{-LL1-}h\}$ four-particle excitations [see Eq. (A17) and discussion in Sec. III)]. Even though $\overline{P^L}$ couples equally to both X amplitudes P_0^L and P_1^L, it dominates the dephasing of P_1^L since the above four-particle excitations have energy comparable to that of X_1. In contrast, X_0 has significantly smaller energy, and thus the broadening of the LL0 peak is mainly determined by the X-phonon interactions. Note that the asymmetric line shape of the LL1 resonance is due to the X-MP states and cannot be obtained within the dephasing time approximation.

We now study the signatures of the X-2DEG correlations in the time and frequency dependence of the transient FWM spectrum. As we discuss below, the correlation effects can be controlled experimentally by varying the central frequency of the optical pulse from LL1 toward LL0. This allows us to control the X amplitudes P_0 and P_1, whose coherent superposition and interactions determine the FWM spectrum. Figure 5 shows the effects of such tuning.

Figure 5(a) shows the FWM spectra when the optical pulse is centered at the LL1 peak, and the LL0 peak is barely excited by the tail of the pulse. For such excitation conditions, we have that $P_0^L \ll P_1^L$, and the photoexcited density of LL1 carriers far exceeds that of LL0 carriers. As a result, the PSF and X-X interaction contributions at the LL0 energy are suppressed as compared to LL1. Despite this, however, the LL0 and LL1 FWM peaks in Fig. 5(a) have comparable heights. To elucidate the physical origin of the nonresonant LL0 FWM signal, we show in Fig. 6 the contributions of PSF, X-X interactions, and MP correlations as a function of time delay.

As clearly seen in the above figure, for optical excitation at the LL1 peak, the LL0 FWM signal is dominated by the MP correlation contribution. At the same time, the LL1 signal is dominated by the PSF contribution. This is shown in

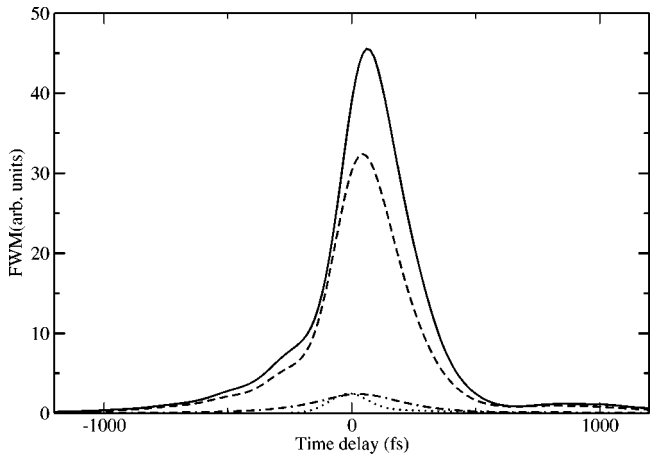

FIG. 6. MP correlation (dashed line), PSF (dotted line), and X-X interaction (dashed-dotted line) contributions to the full FWM signal (full line), calculated at the LL0 peak frequency for photoexcitation as in in Fig. 5(a).

Fig. 7. The origin of the strong MP correlation contribution to the LL0 FWM signal can be seen by comparing the latter for different values of the MP energy Ω_M, while keeping the rest of the parameters constant. As demonstrated in Fig. 8, the LL0 signal, dominated by the MP-mediated LL coupling due to the process of Fig. 3, is *resonantly enhanced* as Ω_M approaches the $X_0 \rightarrow X_1$ excitation energy ($\sim$18 meV here).

One should note here that the X-X interactions also couple the two LL's. However, the corresponding LL0 signal is weaker due to the absence of a resonance, similar to the MP correlation signal for nonresonant Ω_M, and cannot fully account for the strong LL0 signal observed in the experiment of Ref. 30. To see this, note that, in the undoped system, where only the X-X interactions contribute, the FWM signal at the LL0 energy is negligible.[30] More importantly, in the experiment of Ref. 30, the LL0 peak in the doped system was suppressed as compared to the LL1 peak as the density of photoexcited carriers approached that of the 2DEG. In this

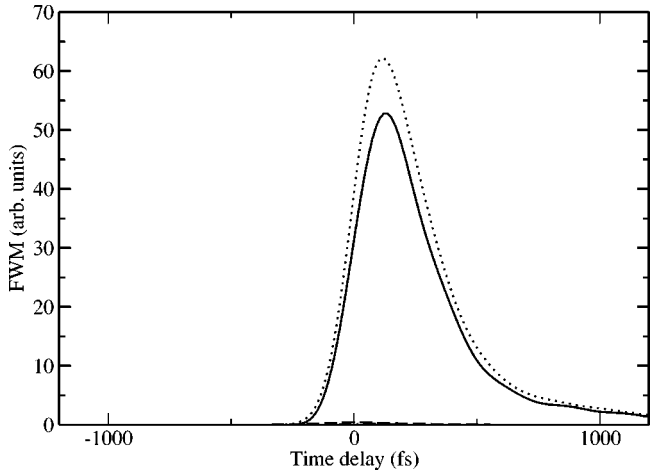

FIG. 7. PSF (dotted line) contribution to the FWM signal (full line) at the LL1 peak frequency for photoexcitation as in Fig. 5(a). The X-X interaction (dashed-dotted line) and MP correlation (dashed line) contributions are negligible here.

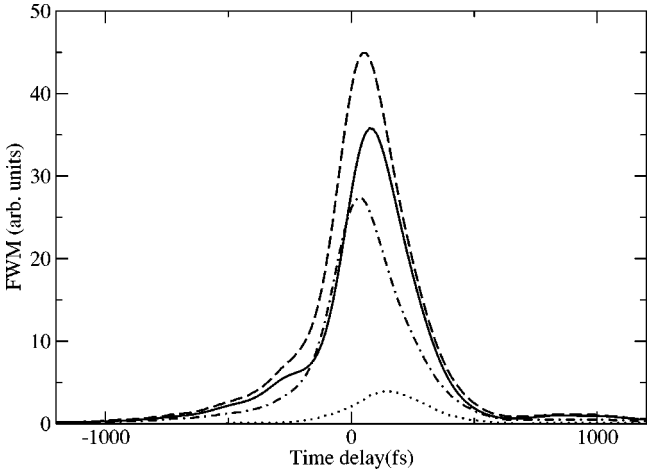

FIG. 8. FWM signal at the LL0 peak frequency for different values of the average MP energy: $\Omega_M = 14$ meV (dotted line), 17 meV (full line), 18 meV (dashed line), and 20 meV (dashed-dotted line). Photoexcitation conditions as in Fig. 5(a).

case the MP correlations of the cold 2DEG diminish, and the doped and undoped QW FWM signals start to look similar.[30]

We now turn to the temporal profile of the FWM signal. Figure 9, which plots the normalized time-dependent LL0 and LL1 signals, demonstrates the difference in the dynamics between the PSF and MP correlation effects that dominate the LL1 and LL0 signals, respectively. As already known from undoped semiconductors, the Pauli blocking effects cannot lead to a FWM signal for negative time delays. The *X*-*X* interactions lead to such a FWM signal, with rise time determined by the dephasing of the interacting *X*-*X* state $|B\rangle$.[2] Within the time-dependent HF approximation,[5] the latter rise time is $\sim(2\Gamma_0+2\Gamma_1)^{-1}$ in the case of interest here.[43] For $\Gamma_0 \sim \Gamma_1$, this rise time is about one-half of the *X*-*X* FWM decay time, $\sim(2\Gamma_1)^{-1}$, or the PSF FWM decay time, $\sim(2\Gamma_0)^{-1}$ at the LL0 energy. Figure 9, however, shows an almost symmetric temporal profile of the LL0 FWM signal, unlike for the LL1 signal. The latter is dominated by the PSF contribution, and is thus suppressed for negative time delays, while the LL0 signal is dominated by the MP correlations, and is enhanced for negative time delays, similar to the experiment of Ref. 30. The origin of this time dependence can be seen from the equation of motion of the MP correlation FWM source term in Eq. (73). After retaining only resonant terms, one can see that the rise of this signal is governed by the time dependence of the product $P_1^L P_0^L$, while the decay is determined by the time dependence of P_1^L, $\mathcal{M}$, and by quantum interference effects. As discussed above, due to the *X*-2DEG scattering, P_1^L dephases much more strongly than P_0^L. Thus the time dependence of $P_1^L P_0^L$ is similar to that of P_1^L, which results in an almost symmetric FWM temporal profile at the LL0 frequency. Furthermore, the quantum interference and beating effects enhance the decay of this signal for positive time delays.

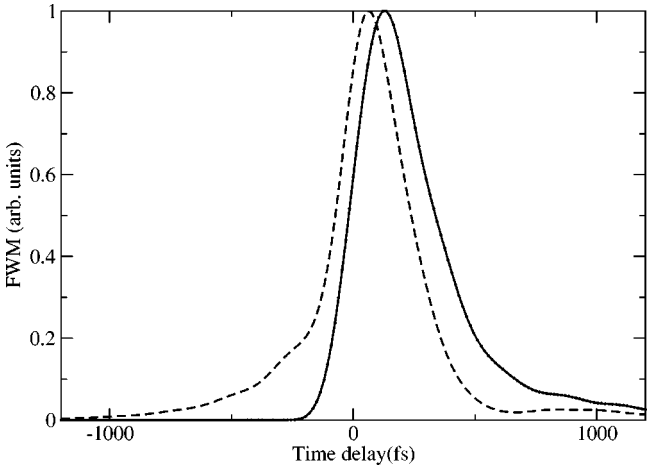

FIG. 9. Temporal profile of the FWM spectrum at the LL0 peak frequency (full line) and the LL1 peak frequency (dashed line). The two signals have been normalized for clarity.

The relative magntitude of the MP correlation versus the PSF/*X*-*X* mean-field FWM signal can be controlled experimentally by changing the central frequency of the optical pulse. Figure 5(b) shows the time-dependent FWM spectrum for excitation conditions such that $|P_0^L| \sim |P_1^L|$. The LL0 signal now dominates, and retains a temporal profile similar to Fig. 5(a). Note that, due to the increased pulse overlap with LL0, the PSF source terms in Eqs. (73) and (74) now have comparable magnitude, while the *X*-*X* interaction and MP correlation source terms are also enhanced. However, the strong dephasing of P_1 discussed above suppresses the LL1 FWM signal. This effect is magnified in the nonlinear spectra as compared to the linear absorption. Importantly, due to the resonant enhancement of Fig. 8, the magnitude of the MP correlation FWM contribution is enhanced more strongly by the increased pulse overlap LL0 with as compared to the mean-field FWM signal. Finally, weak oscillations as a function of time delay, with a period equal to the spacing of the two LL peaks, start to appear.

As can be seen in Figs. 5(c) and 5(d), the oscillations of the LL0 FWM signal, as function of time delay, become more pronounced as the optical excitation frequency is shifted from LL1 towards LL0. It is important to note that the LL1 signal is almost completely suppressed, especially for the excitation frequency of Fig. 5(d), and therefore there are no significant oscillations in the *real time t*, i.e., the time related to the frequency ω via Fourier transform. Thus the oscillations observed in Fig. 5(d), as well as in the experimental data of Ref. 30, have a strong quantum kinetic contribution.[6,7,21] The physical origin of such an effect can be seen by plotting in Fig. 10 the PSF and MP correlation contributions to the LL0 signal as a function of time delay for photoexcitation as in Fig. 5(d). PSF leads to negligible oscillations, while the MP correlation leads to strong oscillations. To see the origin of the latter, we also plot in Fig. 10 the MP correlation signal obtained after neglecting the LL0 coherent density source term $P_0^L P_0^{L*}$ in the equation of motion, Eq. (72), of $\mathcal{M}(t)$; the oscillations diminish in the latter case. To interpret all these, we note that for the excitation conditions of Fig. 5(d), we have $P_0^L \gg P_1^L$, and the density of LL0 carriers far exceeds that of LL1 carriers. In fact, here the PSF contribution exceeds the MP correlation contribution. Most

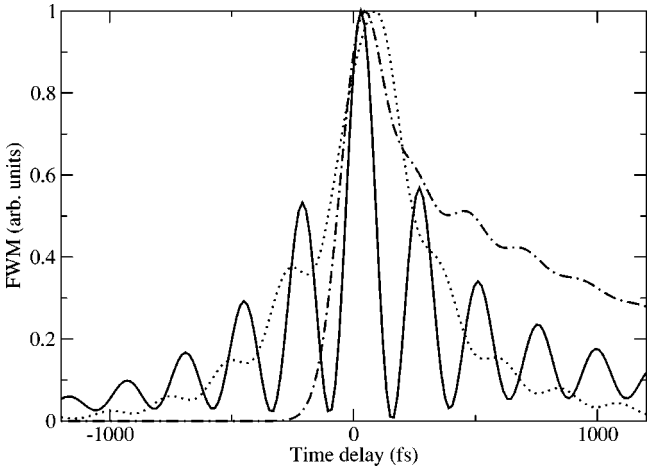

FIG. 10. PSF (dashed-dotted line) and MP correlation (full line) contributions to the FWM signal at the LL0 frequency, normalized to unity for clarity, for photoexcitation as in Fig. 5(d). We also plot the MP correlation signal (dotted line) without the LL0 coherent density source term of $\mathcal{M}(t)$ in Eq. (72). Note the almost complete absence of oscillations in the latter and in the PSF contribution.

importantly, the LL0 coherent density source term of $\mathcal{M}$ is now larger than the source term $P_1^L P_0^{L*}$ that gives the resonant MP contribution. Even though $P_0^L P_0^{L*}$ gives a nonresonant contribution to $\mathcal{M}(t)$, as P_0^L exceeds P_1^L this contribution becomes comparable in magnitude to the resonant contribution due to $P_1^L P_0^{L*}$. The beating between the above two resonant and nonresonant processes gives rise to the strong oscillations. By shifting the excitation frequency further towards LL0, eventually the PSF contribution dominates, and the FWM dephasing is determined by the electron-phonon and intra-LL dephasing processes.[29]

VIII. CONCLUSIONS

In summary, we presented a theory that provides a unified description of the ultrafast nonlinear optical response of a large class of semiconductor systems with a strongly correlated many-electron ground-state. Our main result, Eq. (37), gives the equation of motion for the third-order nonlinear polarization measured in transient wave mixing and pump-probe experiments, and allows us to study the role of the correlations and the interplay between coherent and incoherent effects. Our expansion in terms of the optical field is valid for sufficiently short pulses and/or weak excitation conditions, where the correlations are most pronounced. Our theoretical framework allows us to describe the role of the long-lived collective excitations of a strongly correlated cold electron gas, which is present prior to the optical excitation.

Our theory was applied to the case of the 2DEG in a strong magnetic field. Our numerical solution for photoexcitation close to the LL1 energy with $\sigma^+ - \sigma^+$ circularly polarized light suggests alternative experimental signatures of collective and correlation effects. In this case the relevant 2DEG collective excitations are the long-lived inter-LL magnetoplasmons, which dress the photoexcited magnetoexcitons and lead to polaroniclike effects and strong non-Markovian dephasing. We showed that such effects dominate the time delay and frequency dependence of the transient FWM spectrum. FWM spectroscopy using femtosecond optical pulses provides both the time and the frequency resolution necessary to access this new regime of 2DEG physics. Our theory allowed us to study in a systematic way the experimental signatures of the 2DEG quantum dynamics. We predicted, in particular, a resonant enhancement of the lowest LL FWM signal, a strong dephasing of the next LL magnetoexciton, a symmetric FWM temporal profile, and strong oscillations a as function of time delay with a strong quantum kinetic contribution. Such predicitions agree with recent experimental data.[30]

The above correlation-induced dynamics can be controlled by tuning the central frequency of the optical excitation between the two lowest LL's, which changes the coherent admixture of the two MP-dressed magnetoexcitons, or via coherent control experiments using phase-locked optical pulses.[6] Such experiments, as well as σ^- circularly polarized optical pulses, access the very early dynamics of the strongly correlated 2DEG, during time scales shorter than the duration of the interactions. Such temporal and spectral resolutions open up alternative ways to observe fractional QHE noninstantaneous correlations, as well as magnon, exciton-magnetoroton, charged exciton, and skyrmion effects.

ACKNOWLEDGMENTS

We thank T. V. Shahbazyan and C. Schüller for valuable discussions. This work was supported by the US Department of Energy under Contracts No. DE-AC03-76SF00098 (Berkeley) and DE-FG02-01ER45916 (I.E.P.), and by DARPA/SPINS (I.E.P.).

APPENDIX A

In this appendix we derive some useful expressions for the operators $\hat{Y}_i$, Eq. (22), in the case of the ideal 2D system displaying electron-hole symmetry. To describe the magnetic-field effects, we choose to work in the Landau gauge $\mathbf{A}=(0,Bx,0)$. The eigenstates of the kinetic energy operator are then characterized by the y component of the momentum, k, and the LL index n. The electron eigenstate (ψ_α), and hole eigenstate $(\overline{\psi}_\alpha)$, in this gauge are given by[26,37]

$$\psi_\alpha(\mathbf{r}) = \frac{e^{iky}}{\sqrt{L}} \Psi_n(x - x_k), \overline{\psi}_\alpha(\mathbf{r}) = \psi^*_{-\alpha}(\mathbf{r}), \qquad \text{(A1)}$$

where $\alpha=(k,n,\sigma)$, $-\alpha=(-k,n,\sigma)$, and the spin-σ wave function is kept implicit. In the above equation, Ψ_n is the eigenfunction of the 1D harmonic oscillator with frequency equal to the cyclotron frequency, $x_k = kl^2$ is the x coordinate of the cyclotron orbit center, $l=(\hbar c/eB)^{1/2}$ is the magnetic length (Larmor radius), and L is the system size.[26,37]

The operator $\hat{Y}_i$ is determined by the commutator $[X_i, H_{int}]$, where the Hamiltonian $H_{int}=V_{ee}+V_{hh}+V_{eh}$ describes the Coulomb interactions:

$$H_{int}=\frac{1}{2}\int d\mathbf{r}d\mathbf{r}'v(\mathbf{r}-\mathbf{r}')[\psi^{\dagger}(\mathbf{r})\psi(\mathbf{r})-\overline{\psi}^{\dagger}(\mathbf{r})\overline{\psi}(\mathbf{r})]\times[\psi^{\dagger}(\mathbf{r}')\psi(\mathbf{r}')-\overline{\psi}^{\dagger}(\mathbf{r}')\overline{\psi}(\mathbf{r}')], \quad \text{(A2)}$$

where $\psi^{\dagger}(\mathbf{r})$ is the electron creation operator, $\overline{\psi}^{\dagger}(\mathbf{r})$ is the hole creation operator, and $v(\mathbf{r})$ is the Coulomb potential. By expanding the above creation operators in the Landau basis, we transform the Hamiltonian [Eq. (A2)] into the familiar form

$$H_{int}=\frac{1}{2}\sum_{\alpha_1\alpha_2\alpha_3\alpha_4}[v^{ee}_{\alpha_1\alpha_2,\alpha_3\alpha_4}\hat{e}^{\dagger}_{\alpha_3}\hat{e}^{\dagger}_{\alpha_1}\hat{e}_{\alpha_2}\hat{e}_{\alpha_4}+v^{hh}_{\alpha_1\alpha_2,\alpha_3\alpha_4}\hat{h}^{\dagger}_{\alpha_3}\hat{h}^{\dagger}_{\alpha_1}\hat{h}_{\alpha_2}\hat{h}_{\alpha_4}-v^{eh}_{\alpha_1\alpha_2,\alpha_3\alpha_4}\hat{h}^{\dagger}_{\alpha_3}\hat{e}^{\dagger}_{\alpha_1}\hat{e}_{\alpha_2}\hat{h}_{\alpha_4}-v^{he}_{\alpha_1\alpha_2,\alpha_3\alpha_4}\hat{e}^{\dagger}_{\alpha_3}\hat{h}^{\dagger}_{\alpha_1}\hat{h}_{\alpha_2}\hat{e}_{\alpha_4}], \quad \text{(A3)}$$

where, in the ideal 2D system, the Coulomb interaction matrix elements $v^{ij}_{\alpha_1\alpha_2,\alpha_3\alpha_4}$ (with $i,j=e,h$) are given by

$$v^{ij}_{\alpha_1\alpha_2,\alpha_3\alpha_4}=\int\frac{d\mathbf{q}}{(2\pi)^2}v_qF^{i}_{\alpha_1\alpha_2}(\mathbf{q})F^{j}_{\alpha_3\alpha_4}(-\mathbf{q}), \quad \text{(A4)}$$

where $v_q=2\pi e^2/q$ is the Coulomb potential, and

$$F^{e}_{\alpha_1\alpha_2}(\mathbf{q})=\int d\mathbf{r}\psi^{*}_{\alpha_1}(\mathbf{r})e^{i\mathbf{q}\cdot\mathbf{r}}\psi_{\alpha_2}(\mathbf{r}),$$

$$F^{h}_{\alpha_1\alpha_2}(\mathbf{q})=\int d\mathbf{r}\overline{\psi}^{*}_{\alpha_1}(\mathbf{r})e^{i\mathbf{q}\cdot\mathbf{r}}\overline{\psi}_{\alpha_2}(\mathbf{r}). \quad \text{(A5)}$$

Following Ref. 26, we obtain

$$F^{e}_{\alpha_1\alpha_2}(\mathbf{q})=\varphi_{n_1n_2}(\mathbf{q})f_{k_1k_2}(\mathbf{q})\delta_{\sigma_1,\sigma_2}, \quad \text{(A6)}$$

where

$$f_{k_1k_2}(\mathbf{q})=e^{iq_x(k_1+k_2)l^2/2}\delta_{k_1,k_2+q_y}; \quad \text{(A7)}$$

and for $m\geqslant n$, we have

$$\varphi_{mn}(\mathbf{q})=\frac{n!}{m!}\left[\frac{(-q_y+iq_x)l}{\sqrt{2}}\right]^{m-n}L_n^{m-n}\left(\frac{q^2l^2}{2}\right)e^{-q^2l^2/4}, \quad \text{(A8)}$$

where L_n^{m-n} is the generalized Laguerre polynomial. $\varphi_{mn}(\mathbf{q})$ for $m<n$ can be obtained by using the property

$$\varphi_{mn}(\mathbf{q})=\varphi^{*}_{nm}(-\mathbf{q}). \quad \text{(A9)}$$

Using Eq. (A1) we obtain from Eq. (A5),

$$F^{h}_{\alpha_1\alpha_2}(\mathbf{q})=F^{e}_{-\alpha_2,-\alpha_1}(\mathbf{q}). \quad \text{(A10)}$$

The following symmetry relations can be shown by using the above relations:

$$v^{ij}_{\alpha_1\alpha_2,\alpha_3\alpha_4}=v^{ji}_{\alpha_3\alpha_4,\alpha_1\alpha_2},v^{eh}_{\alpha_1\alpha_2,-\alpha_4-\alpha_3}=v^{ee}_{\alpha_1\alpha_2,\alpha_3\alpha_4},v^{hh}_{-\alpha_4-\alpha_3,\alpha_1\alpha_2}=v^{ee}_{\alpha_3\alpha_4,-\alpha_2-\alpha_1}. \quad \text{(A11)}$$

The commutator $[\hat{h}_{-\alpha}\hat{e}_{\alpha},H_{int}]$ can be calculated from Eq. (A3). Using Eq. (A11) and some algebra, we obtain

$$[\hat{h}_{-\alpha}\hat{e}_{\alpha},H_{int}]=-\sum_{\alpha_1\alpha_2}v^{ee}_{\alpha\alpha_2,\alpha_1\alpha}\hat{h}_{-\alpha_1}\hat{e}_{\alpha_2}+\sum_{\alpha_1\alpha_2\alpha'}[v^{ee}_{\alpha_1\alpha_2,\alpha\alpha'}(\hat{e}^{\dagger}_{\alpha_1}\hat{e}_{\alpha_2}-\hat{h}^{\dagger}_{-\alpha_2}\hat{h}_{-\alpha_1})\hat{h}_{-\alpha}\hat{e}_{\alpha'}-(\alpha\leftrightarrow\alpha')]. \quad \text{(A12)}$$

After summing over k, and recalling definition (4) of the X operators and the definition of $N_{n\sigma}$, the left-hand side of the above equation becomes the commutator $N_{n\sigma}^{1/2}[\hat{X}_{n\sigma},H_{int}]$. Using the properties

$$\sum_k f_{kk_2}(\mathbf{q})f_{k_1k}(-\mathbf{q})=\delta_{k_1k_2} \quad \text{(A13)}$$

and

$$\int d\mathbf{q}v(q)\phi_{nn_2}(\mathbf{q})\phi_{n_1n}(-\mathbf{q})=\delta_{n_1,n_2}\int d\mathbf{q}v(q)|\phi_{nn_1}(\mathbf{q})|^2, \quad \text{(A14)}$$

we obtain after using Eq. (4) and some algebra

$$[\hat{X}_{n\sigma},H_{int}]=-\sum_{n'}V^{0}_{nn'\sigma}(1-\nu_{n'\sigma})\hat{X}_{n'\sigma}+\frac{1}{\sqrt{N_{n\sigma}}}\sum_{\alpha_1\alpha_2}(\hat{e}^{\dagger}_{\alpha_1}\hat{e}_{\alpha_2}-\hat{h}^{\dagger}_{-\alpha_2}\hat{h}_{-\alpha_1})\times\sum_{kk'n'}[v^{ee}_{\alpha_1\alpha_2,knk'n'}\hat{h}_{-kn\sigma}\hat{e}_{k'n'\sigma}-(n\leftrightarrow n')] \quad \text{(A15)}$$

where

$$V^{0}_{nn'\sigma}=\frac{1}{\sqrt{(1-\nu_{n\sigma})(1-\nu_{n'\sigma})}}\int\frac{d\mathbf{q}}{(2\pi)^2}v_q|\phi_{nn'}(q)|^2. \quad \text{(A16)}$$

We now restrict to the first two LL's, which dominate the optical spectra for the excitation conditions of interest. Recalling Eq. (22) we see that the operator $\hat{Y}_n$ is determined by the last term of Eq. (A15). The only nonzero contribution to this term comes from $n'\neq n$, and therefore $n'=1$ if $n=0$, or $n'=0$ if $n=1$. As a result, the rhs of Eq. (A15) changes sign between $n=0$ and $n=1$, and we obtain Eq. (53). The explicit expression for the operator $\hat{Y}_{\sigma}=\sqrt{1-\nu_{1\sigma}}\hat{Y}_{1\sigma}$ can then

be obtained straightforwardly by subtracting the X contributions defined in Eq. (22) from the operator

$$\frac{1}{\sqrt{N}}\sum_{pp'kk'mm'\sigma'}(\hat{e}^{\dagger}_{pm\sigma'}\hat{e}_{p'm'\sigma'}-\hat{h}^{\dagger}_{-p'm'\sigma'}\hat{h}_{-pm\sigma'})\times(v^{ee}_{pmp'm',k1k'0}\hat{h}_{-k1\sigma}\hat{e}_{k'0\sigma}-v^{ee}_{pmp'm',k0k'1}\hat{h}_{-k0\sigma}\hat{e}_{k'1\sigma}). \quad \text{(A17)}$$

The subtracted X contributions describe corrections to the X energies and Coulomb-induced LL coupling due to the 2DEG. As discussed in Sec. VI, for photoexcitation with σ_+ circularly polarized light, we have that $\sigma=\downarrow$. For filling factors close to $\nu=1$, the spin-$\downarrow$ states are empty. We can then decompose Eq. (A17) into the $\sigma'=\downarrow$ term that describes the X-X interactions, and the $\sigma'=\uparrow$ term that mainly describes X-MP interactions.

APPENDIX B

In this appendix we evaluate the HF X-X potentials $\langle B_{ii}|X_jX_{j'}\rangle$ in the ideal 2D system. We consider σ_+ photoexcitation and filling factors close to $\nu=1$ so that Eq. (69) applies. Recalling definition (27), we obtain from Eq. (A17) after using the property $[\hat{X}_i,\hat{X}_j]=0$ that

$$\begin{aligned}\langle B_{1\sigma',n\sigma}| &= \frac{1}{\sqrt{N_{n\sigma}N_{1\sigma'}}}\sum_{pp'kk'n'}[v^{ee}_{pnp'n',k1k'0}\hat{h}_{-pn\sigma}\hat{e}_{p'n'\sigma}\\ &\times\hat{h}_{-k1\sigma'}\hat{e}_{k'0\sigma'}-v^{ee}_{pn'p'n,k1k'0}\hat{h}_{-pn'\sigma}\hat{e}_{p'n\sigma}\\ &\times\hat{h}_{-k1\sigma'}\hat{e}_{k'0\sigma'}-v^{ee}_{pnp'n',k0k'1}\hat{h}_{-pn\sigma}\hat{e}_{p'n'\sigma}\\ &\times\hat{h}_{-k0\sigma'}\hat{e}_{k'1\sigma'}+v^{ee}_{pn'p'n,k0k'1}\\ &\times\hat{h}_{-pn'\sigma}\hat{e}_{p'n\sigma}\hat{h}_{-k0\sigma'}\hat{e}_{k'1\sigma'}]. \quad \text{(B1)}\end{aligned}$$

The only nonzero contribution to the above equation comes from $n'\neq n$. Noting the LL indices, we see that, for the conditions considered here, we have

$$\langle B_{ii}|X_jX_j\rangle=0. \quad \text{(B2)}$$

Substituting the definition of $\hat{Y}_1$ [Eq. (22)], into Eq. (27), restricting to the first two LL's, and denoting $i'\neq i$, we obtain that

$$\begin{aligned}\langle B_{ii}|X_1X_0\rangle &= \langle X_iX_i|H\hat{X}^{\dagger}_1|X_0\rangle-\langle X_i|H\hat{X}_i|X_1X_0\rangle\\ &-\Omega_i\langle X_iX_i|X_1X_0\rangle+V_{ii'}\langle X_1X_0|X_1X_0\rangle\\ &-\langle Y_i|X_i|X_1X_0\rangle. \quad \text{(B3)}\end{aligned}$$

We have $\langle X_iX_i|X_1X_0\rangle=\langle X_iX_i|X_{i'}X_{i'}\rangle=0$ due to the orthogonality of the valence hole states, while $\langle Y_i|\hat{X}_i|X_1X_0\rangle=0$ due to Eq. (69). Using the above, Eq. (22) for the commutator $[H,\hat{X}^{\dagger}_1]$, Eq. (19) for the states $H|X_0\rangle$ and $\langle X_i|H$, and Eq. (B2), we obtain after some algebra that

$$\begin{aligned}\langle B_{ii}|X_1X_0\rangle &= 2V_{ii'}\langle X_1X_0|X_1X_0\rangle-V_{01}\langle X_iX_i|X_0X_0\rangle\\ &-V_{10}\langle X_iX_i|X_1X_1\rangle. \quad \text{(B4)}\end{aligned}$$

Using the relations $\langle X_0X_1|X_1X_0\rangle=1$ and

$$\langle X_iX_i|X_iX_i\rangle=2\left(1-\frac{1}{N_i}\right), \quad \text{(B5)}$$

obtained from Eq. (6), we finally obtain

$$N_i\langle B_{ii}|X_1X_0\rangle=2V_{ii'},\ \ i'\neq i. \quad \text{(B6)}$$

The above relation recovers the results of Ref. 43.

APPENDIX C

In this appendix we derive some useful relations for the overlap $\langle 2\text{DEG}^*|M_{ii'}\rangle$, where $|2\text{DEG}^*\rangle$ is any 2DEG excited state, for filling factors close to $\nu=1$ and for σ_+ polarized light. Using Eqs. (32) and (53), we obtain

$$N_0^{1/2}|M_{0i}\rangle=N_0^{1/2}\hat{Y}_0\hat{X}^{\dagger}_i|0\rangle=-N_1^{1/2}\hat{Y}_1\hat{X}^{\dagger}_i|0\rangle=-N_1^{1/2}|M_{1i}\rangle. \quad \text{(C1)}$$

From Eq. (32) we obtain after using Eq. (22),

$$\begin{aligned}|M_{ii'}\rangle &= \hat{X}_i|Y_{i'}\rangle-(H+\Omega_i-\Omega_{i'})\hat{X}_i|X_{i'}\rangle\\ &+\sum_{j\neq i}V_{ij}\hat{X}_j|X_{i'}\rangle-\sum_{j\neq i}V_{ji'}\hat{X}_i|X_j\rangle. \quad \text{(C2)}\end{aligned}$$

The state $\hat{X}_i|Y_{i'}\rangle$ describes a 2DEG excitation, created via the process shown in the first three panels of Fig. 3. Using Eq. (69) and the property $\langle 2\text{DEG}^*|H|0\rangle=0$, we obtain

$$\langle 2\text{DEG}^*|M_{ii'}\rangle=\langle 2\text{DEG}^*|\hat{X}_i|Y_{i'}\rangle. \quad \text{(C3)}$$

Using Eq. (53,) we then obtain

$$\begin{aligned}N_0^{1/2}\langle 2\text{DEG}^*|M_{i0}\rangle &= N_0^{1/2}\langle 2\text{DEG}^*|\hat{X}_i|Y_0\rangle\\ &=-N_1^{1/2}\langle 2\text{DEG}^*|\hat{X}_i|Y_1\rangle\\ &=-N_1^{1/2}\langle 2\text{DEG}^*|M_{i1}\rangle. \quad \text{(C4)}\end{aligned}$$

[1] D.S. Chemla and J. Shah, Nature (London) **411**, 549 (2001).
[2] D. S. Chemla, in *Nonlinear Optics in Semiconductors*, edited by R. K. Willardson and A. C. Beers (Academic, New York, 1999).
[3] J. Shah, *Ultrafast Spectroscopy of Semiconductors and Semiconductor Nanostructures* (Springer, Heidelberg, 1999).
[4] S. Mukamel, *Principles of Nonlinear Optical Spectroscopy* (Oxford University Press, Oxford, 1995).
[5] H. Haug and S. W. Koch, *Quantum Theory of the Optical and Electronic Properties of Semiconductors*, 2nd ed. (World Scientific, Singapore, 1993).
[6] M. Wegener and D.S. Chemla, Chem. Phys. **251**, 269 (2000).
[7] H. Haug and A.-P. Jauho, *Quantum Kinetics in Transport and Optics of Semiconductors* (Springer, New York, 1996).
[8] V.M. Axt and S. Mukamel, Rev. Mod. Phys. **70**, 145 (1998).
[9] I.E. Perakis and T.V. Shahbazyan, Surf. Sci. Rep. **40**, 1 (2000); Int. J. Mod. Phys. B **13**, 869 (1999); I.E. Perakis, Chem. Phys. **210**, 259 (1996).
[10] V.M. Axt and A. Stahl, Z. Phys. B: Condens. Matter **93**, 195 (1994).
[11] V.M. Axt, K. Victor, and A. Stahl, Phys. Rev. B **53**, 7244 (1996).
[12] Th. Östreich, K. Schönhammer, and L.J. Sham, Phys. Rev. B **58**, 12 920 (1998).
[13] S. Louie, in *Computational Materials Sciences*, edited by C. Y. Fong (World Scientific, Singapore, 1998).
[14] L.J. Sham, Phys. Rev. **150**, 720 (1966).
[15] W. Schäfer, D.S. Kim, J. Shah, T.C. Damen, J.E. Cunningham, K.W. Goossen, L.N. Pfeiffer, and K. Kohler, Phys. Rev. B **53**, 16 429 (1996).
[16] I.E. Perakis and D.S. Chemla, Phys. Rev. Lett. **72**, 3202 (1994); I.E. Perakis, I. Brener, W.H. Knox, and D.S. Chemla, J. Opt. Soc. Am. B **13**, 1313 (1996).
[17] T.V. Shahbazyan, N. Primozich, I.E. Perakis, and D.S. Chemla, Phys. Rev. Lett. **84**, 2006 (2000); N. Primozich, T.V. Shahbazyan, I.E. Perakis, and D.S. Chemla, Phys. Rev. B **61**, 2041 (2000).
[18] D.-S. Kim, J. Shah, J.E. Cunningham, T.C. Damen, S. Schmitt-Rink, and W. Schäfer, Phys. Rev. Lett. **68**, 2838 (1992).
[19] H. Wang, J. Shah, T.C. Damen, S.W. Pierson, T.L. Reinecke, L.N. Pfeiffer, and K. West, Phys. Rev. B **52**, R17 013 (1995).
[20] I. Brener, W.H. Knox, and W. Schaefer, Phys. Rev. B **51**, 2005 (1995).
[21] Q.T. Vu, H. Haug, W.A. Hügel, S. Chatterjee, and M. Wegener, Phys. Rev. Lett. **85**, 3508 (2000).
[22] S. Bar-Ad, I. Bar-Joseph, Y. Levinson, and H. Shtrikman, Phys. Rev. Lett. **72**, 776 (1994).
[23] T. Chakraborty and P. Pietiläinen, *The Quantum Hall Effects, Fractional and Integral*, 2nd ed. (Springer, New York, 1995).
[24] H.L. Stormer, D.C. Tsui, and A.C. Gossard, Rev. Mod. Phys. **71**, S298 (1999).
[25] C. Kallin and B.I. Halperin, Phys. Rev. B **30**, 5655 (1984).
[26] A.H. MacDonald, J. Phys. C **18**, 1003 (1985).
[27] G. Finkelstein, H. Shtrikman, and I. Bar-Joseph, Phys. Rev. B **56**, 10 326 (1997).
[28] G. Yusa, H. Shtrikman, and I. Bar-Joseph, Phys. Rev. Lett. **87**, 216402 (2001).
[29] N.A. Fromer, C. Schüller, D.S. Chemla, T.V. Shahbazyan, I.E. Perakis, K. Maranowski, and A.C. Gossard, Phys. Rev. Lett. **83**, 4646 (1999).
[30] N.A. Fromer, C.E. Lai, D.S. Chemla, I.E. Perakis, D. Driscoll, and A.C. Gossard, Phys. Rev. Lett. **89**, 067401 (2002); N. A. Fromer, C. Schüller, C. E. Lai, D. S. Chemla, I. E. Perakis, D. Driscoll, and A. C. Gossard, Phys. Rev. B **66** 205314 (2002); I. E. Perakis and D. S. Chemla, Phys. Status Solidi B **234**, 242 (2002).
[31] R. Merlin (private communication).
[32] For a review of quantum Hall ferromagnets, see, e.g., S. M. Girvin and A. H. MacDonald, in *Novel Quantum Liquids in Low Dimensional Semiconductor Structures*, edited by S. Das Sarma and A. Pinczuk (Wiley, New York, 1996).
[33] E.H. Aifer, B.B. Goldberg, and D.A. Broido, Phys. Rev. Lett. **76**, 680 (1996).
[34] See, e.g., P. Hawrylak and M. Potemski, Phys. Rev. B **56**, 12 386 (1997); N.R. Cooper and D.B. Chklovskii, *ibid.* **55**, 2436 (1997).
[35] P. Kner, S. Bar-Ad, M.V. Marquezini, D.S. Chemla, and W. Schäfer, Phys. Rev. Lett. **78**, 1319 (1997); P. Kner, W. Schäfer, R. Lövenich, and D.S. Chemla, *ibid.* **81**, 5386 (1998); P. Kner, S. Bar-Ad, M.V. Marquezini, D.S. Chemla, R. Lövenich, W. Schäfer, Phys. Rev. B **60**, 4731 (1999).
[36] T.V. Shahbazyan, N. Primozich, and I.E. Perakis, Phys. Rev. B **62**, 15 925 (2000).
[37] J. Schilp, T. Kuhn, and G. Mahler, Phys. Rev. B **50**, 5435 (1994).
[38] V. Chernyak, S. Yokojima, T. Meier, and S. Mukamel, Phys. Rev. B **58**, 4496 (1998).
[39] N.A. Fromer, P. Kner, D.S. Chemla, R. Lövenich, and W. Schäfer, Phys. Rev. B **62**, 2516 (2000).
[40] A. Pinczuk, J.P. Valladares, D. Heiman, A.C. Gossard, J.H. English, C.W. Tu, L. Pfeiffer, and K. West, Phys. Rev. Lett. **61**, 2701 (1988).
[41] M. Levenson, *Introduction to Nonlinear Laser Spectroscopy* (Academic Press, New York, 1982).
[42] C. Stafford, S. Schmitt-Rink, and W. Schaefer, Phys. Rev. B **41**, 10 000 (1990).
[43] R. Haydock, Solid State Phys. **35**, 215 (1980); K. Ohno, K. Esfarjani, and Y. Kawazoe, *Computational Materials Science* (Springer-Verlag, Berlin, 1999).
[44] H. Chu and Y.-C. Chang, Phys. Rev. B **39**, 10 861 (1989).
[45] S.R. Bolton, U. Neukirch, L.J. Sham, D.S. Chemla, and V.M. Axt, Phys. Rev. Lett. **85**, 2002 (2000); V.M. Axt, S.R. Bolton, U. Neukirch, L.J. Sham, and D.S. Chemla, Phys. Rev. B **63**, 115303 (2001).
[46] I.K. Marmorkos and S. Das Sarma, Phys. Rev. B **45**, 13 396 (1992).